After the antibiotic era: effect of Nanostructured Lipid Carriers against *Helicobacter pylori* biofilms

Ana Sofia Ferreira Leite de Pinho

Master Thesis for the degree in Master of Science in Bioengineering,

specialization in Molecular Biotechnology

Supervisor:

PhD Paula Parreira

i3S - Instituto de Investigação e Inovação em Saúde, Universidade do Porto, Portugal

BioEngineered Surfaces, INEB – Instituto de Engenharia Biomédica, Portugal

Co-supervisors:

PhD Catarina Leal Seabra

LAQV, REQUIMTE, Laboratório de Química Aplicada, Faculdade de Farmácia da Universidade do Porto, Portugal

PhD M. Cristina Martins

i3S - Instituto de Investigação e Inovação em Saúde, Universidade do Porto, Portugal

BioEngineered Surfaces, INEB – Instituto de Engenharia Biomédica, Portugal

November 2020

"All human wisdom is summed up in these two words:
wait and hope"

Emily Dickinson

Abstract

Helicobacter pylori (*H. pylori*) is one of the most successful human pathogens. It colonizes more than half of the world's population stomach and is associated with the development of gastric cancer, the 5th with the highest incidence and the 3rd with the highest mortality worldwide. Despite an intensive treatment regimen with two or more antibiotics conjugated with proton pump inhibitors, the total eradication of infection by *H. pylori* does not occur in approximately 40% of cases.

Among the possible causes that account for treatment failure is the ability of this gastric pathogen to form biofilms, as these structures have been correlated with increased resistance to therapies.

The potential of nanostructured lipid carriers (NLC) against *H. pylori* infection has been previously demonstrated. Due to their ability to kill planktonic bacteria, the goal of the present work was to explore their effect against *H. pylori* when organized in a biofilm.

Unloaded (U-NLC) and docosahexaenoic acid-loaded NLC (DHA-NLC) were produced by hot homogenization and ultrasonication using a blend of lipids (Miglyol®-812 and Precirol® ATO5) and a surfactant (Tween® 60). Characterization by dynamic light scattering (DLS) and electrophoretic light scattering (ELS) showed monodisperse suspensions with nanoparticles with diameters of approximately 255±16 nm and 346±23 nm and surface charge of approximately -32±2 mV and -21±1 mV, for U-NLC and DHA-NLC, respectively.

To establish an *H. pylori* model of mature biofilms, it was required to first optimize its growth conditions. The final settings selected were 3 days of growth in culture media supplemented with a sub-optimal concentration of fetal bovine serum (FBS). The mature *H. pylori* biofilms were then characterized regarding total biofilm biomass and number of viable bacteria.

The effect of NLC against *H. pylori* biofilms were assessed by quantification of total biofilm biomass and the number of viable bacteria, as well as biofilm visualization by scanning electron microscopy (SEM) and confocal laser scanning microscopy (CLSM). Both U- and DHA-NLC prevented further growth of the biofilm (inhibition) and reduced its biomass. Nonetheless, DHA-NLC had effect at lower concentrations when compared to U-NLC (0.156% v/v (i.e. NLC suspension/total volume) versus 1.25% v/v for U-NLC). Regarding *H. pylori* viability, the minimal bactericidal concentration (MBC) for planktonic bacteria, as well as the biofilm bactericidal concentration (BBC) concerning bacteria embedded in the biofilm were established at a concentration of 0.156% v/v. Despite the lack of viable bacteria in colony-forming unit (CFU) counting for most of the NLC concentrations tested, CLSM imaging highlighted that not all of the bacteria were dead, having suffered a transition into a coccoid shape and possibly to a viable but non-culturable (VBNC) state.

Overall, NLC show great promise as a treatment for *H. pylori* infection, being able to target and significantly reduce the number of viable bacteria embedded in the biofilm matrix, even at low concentrations.

Acknowledgements

I find it hard to believe that a person can write a Master Thesis alone. For me, it took a village and I am very thankful to all of you:

Prof. Dr. Cristina Martins, for helping me start my journey in research in the most amazing group in the world, the Bioengineered Surfaces Group, and for all the support as the group leader and co-supervisor.

Dr. Paula Parreira, for the guidance throughout my Master's Project and Thesis, for answering all my calls and messages and, above all, for the encouragement and for reminding me that "this is MY work and I should be proud of it".

Dr. Catarina Seabra, my very first supervisor, who never left my side even when she left the group, for teaching me all of the little and big things about working in a lab and for her constant energy and enthusiasm.

Prof. Dr. Salette Reis and Dr. Cláudia Nunes, for all the support and help at Faculdade de Farmácia.

The teachers in MIB, for making it the most challenging but also the most rewarding degree, for all the knowledge shared and opportunities that were given.

The members of the Bioengineered Surfaces Group, for being so welcoming and friendly, for all the constant support and for finding a lot of excuses to eat cake.

The Pylordes and Burrata, for making all of this work more bearable, for being there when everyone abandoned me to go on Erasmus, and for all the good food we shared and will share in the future.

The friends I made in MIB and specially the Biotech group, for all the good moments and the companionship.

Bia, Beni and Tó, you hold a special place in my heart, the biggest thank you for always listening to me, for making me laugh and for being the best friends anyone could ever ask for.

My family, for being my refuge and my rock, for all of the affection and help when it was most needed.

My dear parents, for all of your love and support throughout my 23 years on this Earth, for always pushing me to do my best and celebrating the rewards it brought into my life. And Rafe, my beautiful cat, for being the perfect distraction when I needed a break from writing, and for welcoming me home when I arrived after working all day.

And God, for giving me all of these people and the strength needed to accomplish this.

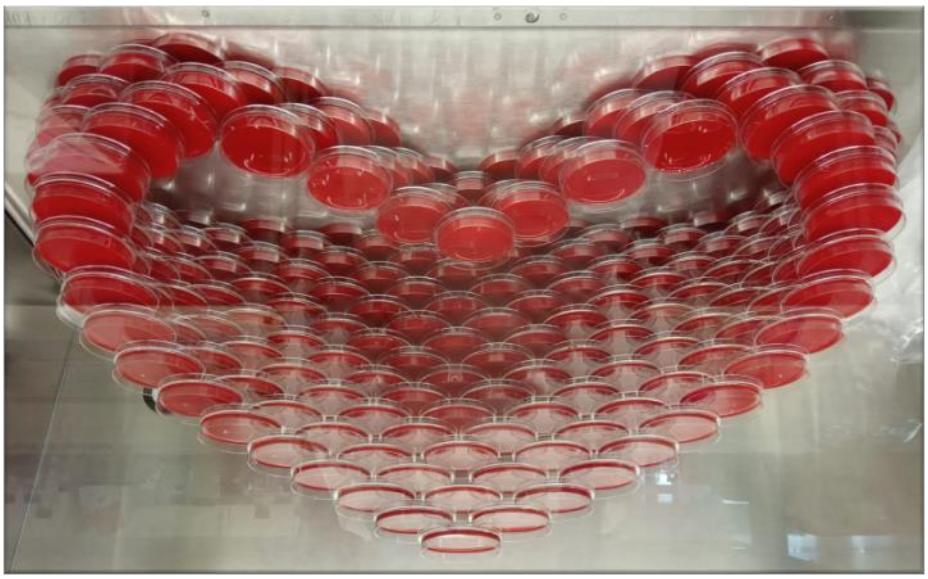

This work was supported by Fundo Europeu de Desenvolvimento Regional (FEDER) funds through the COMPETE 2020, Operational Program for Competitiveness and Internationalization (POCI), Portugal 2020 and NORTE-01-0145-FEDER-000012 and by Fundação para a Ciência e a Tecnologia (FCT)/Ministério da Ciência, Tecnologia e Inovação funds through the POCI-01-0145-FEDER-007274, PyloriBinders - Helicobacter pylori specific biomaterials for antibiotic-free treatment/diagnostic of gastric infection (PTDC/CTM-BIO/4043/2014).

Table of Contents

List of figures

List of tables

Abbreviations

AlpA/B	Adherence-associated lipoproteins A/B
AMX	Amoxicillin
BabA/B/C	Blood-group Antigen Binding adhesins A/B/C
BB	Brucella broth
BBC	Biofilm Bactericidal Concentration
BS	Bismuth salts
CagA	Cytotoxin-associated gene A
CFU	Colony-forming Unit
CLR	Clarithromycin
CLSM	Confocal Laser Scanning Microscopy
CV	Crystal Violet
DHA	Docosahexaenoic acid
DHA-NLC	Docosahexaenoic acid-loaded Nanostructured Lipid Carrier
DLS	Dynamic Light Scattering
DMSO	Dimethyl Sulfoxide
DOX	Doxycycline
ELS	Electrophoretic Light Scattering
EPS	Extracellular Polymeric Substances
FBS	Fetal Bovine Serum
FZ	Furazolidone
HopZ	*Helicobacter* outer membrane protein Z
HPC	High-pressure homogenization
H. pylori	*Helicobacter pylori*
HtrA	High-temperature requirement protein A
LPS	Lipopolysaccharide
LVX	Levofloxacin
MAG	Multifocal Atrophic Gastritis
MBC	Minimal Bactericidal Concentration
MBEC	Minimal Biofilm Eradication Concentration
MBIC	Minimal Biofilm Inhibitory Concentration
MIC	Minimal Inhibitory Concentration

MTZ	Metronidazole
MXF	Moxifloxacin
NAG	Non-Atrophic Gastritis
NLC	Nanostructured Lipid Carriers
NTA	Nanoparticle Tracking Analysis
OD	Optical Density
OipA	Outer inflammatory protein A
OMP	Outer membrane protein
PBS	Phosphate-buffered Saline
PCR	Polymerase chain reaction
PdI	Polydispersity index
PEG	Polyethylene glycol
PFA	Paraformaldehyde
PI	Propidium Iodide
PLA2	Phospholipase A2
PNA-FISH	Peptide nucleic acid fluorescence *in situ* hybridization
PPI	Proton Pump Inhibitor
RFB	Rifabutin
RNA	Ribonucleic acid
RPM	Revolutions per minute
SabA/B	Sialic Acid Binding adhesins A/B
SEM	Scanning Electron Microscopy
SLN	Solid Lipid Nanoparticles
TET	Tetracycline
T4SS	Type IV Secretion System
TSA	Trypticase Soy agar
U-NLC	Unloaded Nanostructured Lipid Carrier
VacA	Vacuolating cytotoxin A
VBNC	Viable but non-culturable
ZP	Zeta potential

Chapter 1 - Introduction

1.1. *Helicobacter pylori*

Helicobacter pylori is a Gram-negative, microaerophilic (<5% O_2) bacterium, measuring 2 to 4 μm in length and 0.5 to 1 μm in width. It is typically spiral-shaped (**Figure 1.1**) but, as a survival strategy under adverse conditions (e.g. lack of nutrients, high oxygen concentration), it can convert to a rod- or coccoid shape (1).

Figure 1.1 - Scanning electron microscope photograph of *Helicobacter pylori*. In (2).

It was first successfully isolated in 1982 by J. Robin Warren and Barry Marshall and, at the time, they stated that "these bacteria do not fit in any known species either morphologically or biochemically", although some similarities indicated that they might belong to the genus *Campylobacter* (3). As such, they were first designated *Campylobacter pylori*, but further studies uncovered specific structure and genetic differences that led to the creation of the new genus *Helicobacter*, changing these bacteria's classification to *Helicobacter pylori* (4).

Furthermore, in 1994, *H. pylori* was classified as a class I carcinogen by the International Agency for Research on Cancer due to its unequivocal association with gastric cancer (5). Currently, this type of cancer has the 5th highest incidence and the 3rd highest mortality rate worldwide, being estimated that *H. pylori* infection is responsible for up to 89% of this cancer's global burden (6, 7).

While infection usually occurs at a young age, many individuals remain asymptomatic or might only develop symptoms later in life (8). When symptoms manifest, they are a result of the progression of the infection through a series of histological changes known as the Correa's precancerous cascade of events (**Figure 1.2**). It starts with chronic non-atrophic gastritis (NAG), followed by precursor lesions of gastric cancer such as multifocal atrophic gastritis (MAG), intestinal

metaplasia, dysplasia and, finally, 1-3% of infected individuals, will progress to develop invasive gastric carcinoma (9, 10).

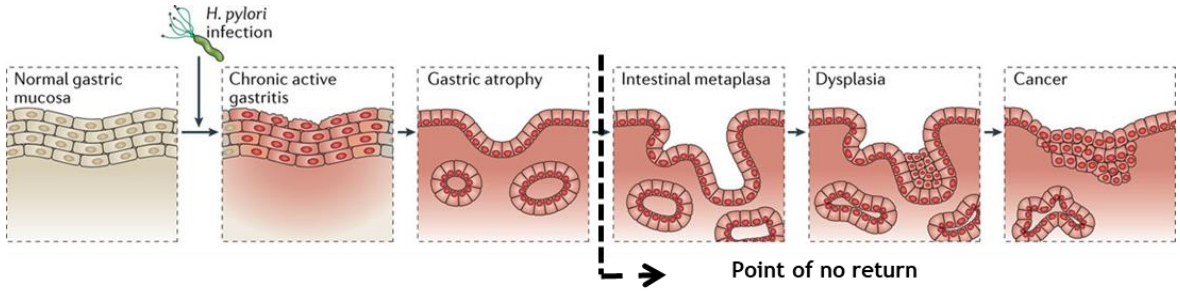

Figure 1.2 - Alterations in the gastric mucosa from normal to gastric cancer after infection by *H. pylori*, as proposed by Correa *et al*. The stage at which the changes caused by the infection become irreversible despite the elimination of the pathogen is represented as the point of no return. Adapted from (11).

H. pylori has the ability to modulate inflammatory processes to intensify its pathogenicity (12). Also, it can influence the autophagy pathway of the host, stimulating both apoptosis and cell division of epithelial cells together with the induction of oncogenic mutations (8, 13). Nonetheless, the outcome of the infection is a complex interplay and depends on various factors such as the host genetic susceptibility, lifestyle and environment, as well as the strain's virulence characteristics (8, 14).

1.1.1. Epidemiology

H. pylori is one of the most successful pathogens, infecting approximately half of the world's population. The global prevalence of infection is illustrated in **Figure 1.3**.

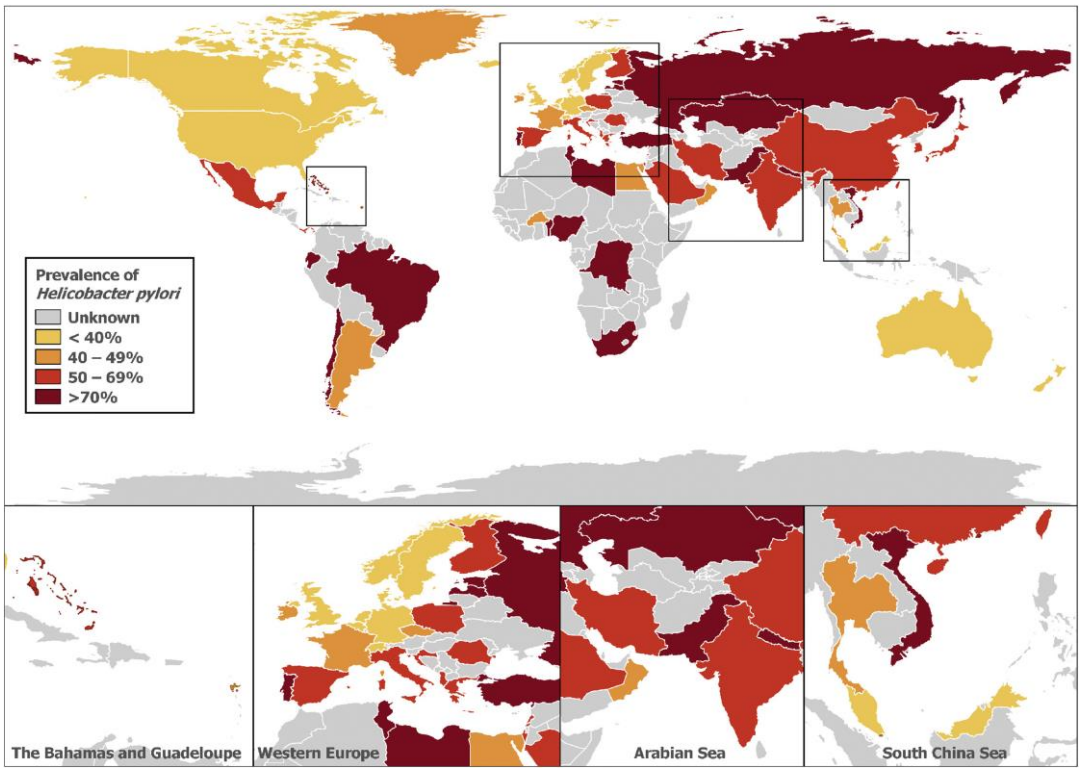

Figure 1.3 - Global prevalence of *H. pylori* infection. Prevalence is highest in Africa and Latin America, followed by Asia and Europe and lowest in North America and Oceania. In (15).

Although the worldwide prevalence is approximately 44%, developing countries such as Nigeria (89.7%) and South Africa (86.8%) have some of the highest rates and an estimated prevalence of nearly 80%, while in industrialized countries it remains under 40%, with rates as low as 11% and 15% in Belgium and Sweden, respectively (16). Interestingly, numbers among countries with similar living conditions still show great disparities, reflecting the complex interplay between *H. pylori*, host factors and external factors. For instance, in 2013 Portugal had one of the highest rates for the prevalence of *H. pylori* infection in Western Europe, reaching 84.2%, despite similar development status and levels of sanitation when compared to other European countries (17-19).

The main routes of *H. pylori* transmission are thought to be person-to-person and environmental contaminations, through the ingestion of contaminated water and food (14, 20, 21). Acquisition of infection via the zoonotic route is still argued with transmission being feasible but, to date, no animal has been proven as a reservoir for these bacteria (22, 23).

Some risk factors may increase the probability of infection, namely: lower socioeconomic status, poor hygiene practices, crowded families, absence of drinking water, inappropriate handling of food and the absence of proper sewage disposal (20).

1.1.2. The keys to have a successful pathogen

The gastric environment presents many challenges for microbial colonization, such as an acidic pH (pH=1.5 to 3.5 in the gastric lumen), peristalsis, mucus flow and mucosal cell turnover (24). *H. pylori* uses different mechanisms to adapt to these conditions and colonize a protected niche on the surface of epithelial cells in the stomach's antral region (**Figure 1.4**) (1).

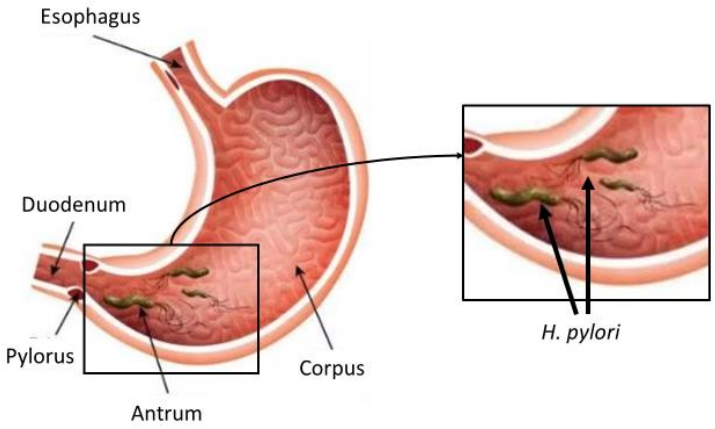

Figure 1.4 - *H. pylori* residing in the antral region of the stomach. Adapted from (25).

As a Gram-negative, the *H. pylori* cell wall is comprised of an outer and an inner membrane separated by an approximately 30 nm thick periplasm (**Figure 1.5**). Also, its peptidoglycan has a unique composition, being extremely rich in muropeptides. Other features that distinguish *H. pylori* from other bacterial pathogens are its unusual cellular fatty acid and lipid profile, including a high content of cholesterol glucosides (25% of total lipid content, by weight) and its lipopolysaccharide (LPS) mimicry of Lewis antigens (26-28).

Besides the above-mentioned characteristics, *H. pylori* is able to convert into a viable but non-culturable (VBNC) state as a defense from environmental stressors (e. g. insufficient nutrients, oxygen, sub-inhibitory antibiotic concentrations). In this state, bacterial cells change their morphology, converting from a bacillar shape into a coccoid shape, suffer changes in metabolism, cell wall composition and gene expression. An outcome of some of these changes is the inability to detect these cells by conventional culture techniques but still they remain infective (29, 30).

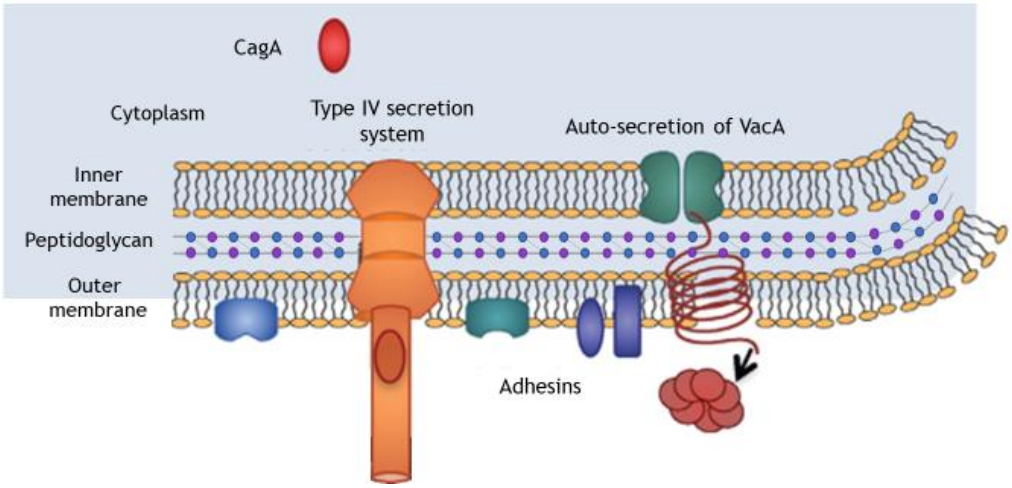

Figure 1.5 - *H. pylori* cell wall and virulence factors. Adapted from (31).

Together with these characteristics, the most important virulence factors that account for the success of this gastric pathogen are summarized in **Table 1.1** and will be briefly discussed over the next subsections.

Table 1.1 – *H. pylori* virulence factors and their function.

Virulence factor	Function
Flagella	Bacterial motility, colonization of the gastric mucosa
Outer membrane proteins	Adherence to mucins and gastric epithelial cells
Urease	Maintenance of a pH-neutral microenvironment
Heat shock proteins	Protection of essential cell components from various types of stress
Lewis antigens	Immune evasion
CagA	Alteration of cell signaling, alteration of cell-cell connections, proinflammatory
VacA	Formation of vacuoles, induction of apoptosis
Superoxidase dismutase	Defense against the immune system
Catalase	Defense against the immune system

Flagella

Each bacterium has 2 to 6 unipolar-sheathed flagella, approximately 3 μm long that provide motility. Also, the bacteria's spiral morphology allows *H. pylori* to move in a screw-like manner, enabling its penetration in the mucus layer overlying the gastric epithelial cells, escaping the harsh settings of the lumen (1, 32). The majority of *H. pylori* cells are found within the mucus layer or adhered to gastric epithelial cells and always less than 25 μm away from the stomach surface (24, 33).

Outer membrane proteins

Outer membrane proteins are responsible for mediating bacterial adherence to gastric epithelial cells. These include blood group antigen-binding adhesins (BabA/B/C), sialic acid-binding adhesins (SabA/B), adherence-associated lipoproteins (AlpA/B), the outer inflammatory protein (OipA) and the *Helicobacter* outer membrane protein Z (HopZ) (14, 34, 35). *H. pylori* also produce phospholipase A2 (PLA2), a protein able to promote adherence to mucins and specifically bind to the epithelial cells of the gastric mucosa (36).

Urease

The production of the enzyme urease allows *H. pylori* chemotaxis and the maintenance of a pH-neutral microenvironment surrounding the bacteria in the acidic environment of the stomach, which is typically unfavorable for bacterial growth (**Figure 1.6**). The inability to produce urease is a characteristic in mutant *H. pylori* that prevents it from colonizing the gastric mucosa (13).

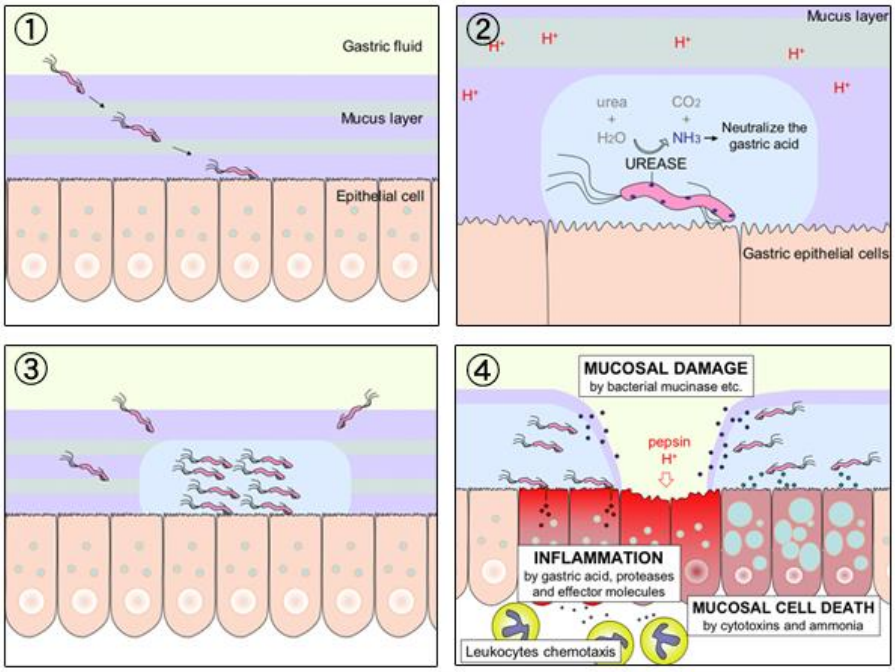

Figure 1.6 - Role of urease in the colonization of gastric mucosa by *H. pylori*. Panel numbers denote successive stages in the colonization of the host mucosa. (1) Attachment is followed by (2) formation and activity of extracellular urease (black dots). This leads to (3) aggregation and (4) mucosal cell damage. In (37).

Heat shock proteins

To increase the bacteria's chance of survival in this extreme environment, the presence of heat shock proteins is essential as they play a protective role against stressors, such as elevated temperature, pH changes and osmotic shock. An example is the high-temperature requirement A (HtrA), a secreted serine protease associated with the maintenance of important periplasmic and outer membrane proteins by refolding or degrading misfolded proteins (38).

Lewis antigens

H. pylori has developed strategies to evade the immune system and even to manipulate it. *H. pylori* LPS is able to mimic Lewis antigens, which resemble human blood group antigens. By expressing antigens analogous to the ones expressed by the host, it can avoid immune recognition

(39). Molecular mimicry of Lewis antigens has yet another function: the presence of these epitopes, which are shared with the host cells, can lead to the formation of autoantibodies and induce further tissue damage (40).

VacA and CagA

Some *H. pylori* strains encode genes to produce toxins, namely the cytotoxin-associated gene A protein (CagA) and the vacuolating cytotoxin A (VacA). CagA is an oncoprotein that enters the epithelial cells via a type IV secretion system (T4SS). It induces various transcription factors involved in essential cellular activities, alters the morphology of the cells, interacts with the protein E-cadherin, breaking connections between the gastric epithelial cells and has a proinflammatory effect by stimulating the secretion of interleukin-8 (35, 41). VacA is a cytotoxin that leads to the production of vacuoles in gastric epithelial cells that lead to apoptosis. The presence or absence of VacA and CagA in clinical strains divides them into two types according to infection severity: type 1 strains, expressing both VacA and CagA, are more severe and associated with a poorer prognosis than type 2 strains, which do not express VacA or CagA (8).

Superoxidase dismutase and catalase

Cytoplasmic proteins such as the enzymes superoxide dismutase and catalase play important roles in protecting *H. pylori* from oxidative stress, derived both from metabolism and the host immune response. Superoxide dismutase and catalase hinder the immune response by breaking down superoxide anions and hydrogen peroxide, respectively (32, 42).

1.1.3. Current Treatment

The use of a single antibiotic (monotherapy) is not enough for the eradication of *H. pylori* infection. Although these bacteria present susceptibility to several antibiotics when tested *in vitro*, eradication rates *in vivo* are significantly lower. Also, for an infection with tendency for recalcitrance due to antibiotic resistance, monotherapy shows little promise (43).

In addition, there is not a standardized therapy for *H. pylori* infection. Treatment selection can differ depending on the doctor prescribing it, geographic trends/patterns in antibiotic resistance, previous treatments for other infections and/or *H. pylori* and allergies, among others (43). Usually, the standard treatment consists of 7 to 14 days of administration of a proton pump inhibitor (PPI) together with 2 antibiotics. The PPI works as an acid suppressant, increasing the gastric pH and, as a result, improves the efficacy of some antibiotics by stabilizing them and preventing bioactivity loss. The PPI also has anti-urease and anti-ATPase properties (44). Amoxicillin, clarithromycin and metronidazole are the most commonly used antibiotics (43, 45). It is heavily recommended that, if the first therapeutical attempt fails, the following treatments should avoid previously used antibiotics, as it leads to poor eradication rates. Also, third-line and subsequent treatments should be formulated only after performing antimicrobial susceptibility tests (46).

Currently, the cure rates obtained with the different therapies for *H. pylori* infection are mostly under the 80% threshold limit defined by the Maastricht consensus group, which separates acceptable from unacceptable treatment results (47, 48). Indeed, due to several factors, treatment still fails to relieve patients of the infection in approximately 40% of cases (49, 50).

The most common therapies and respective eradication rates are shown in **Figure 1.7**.

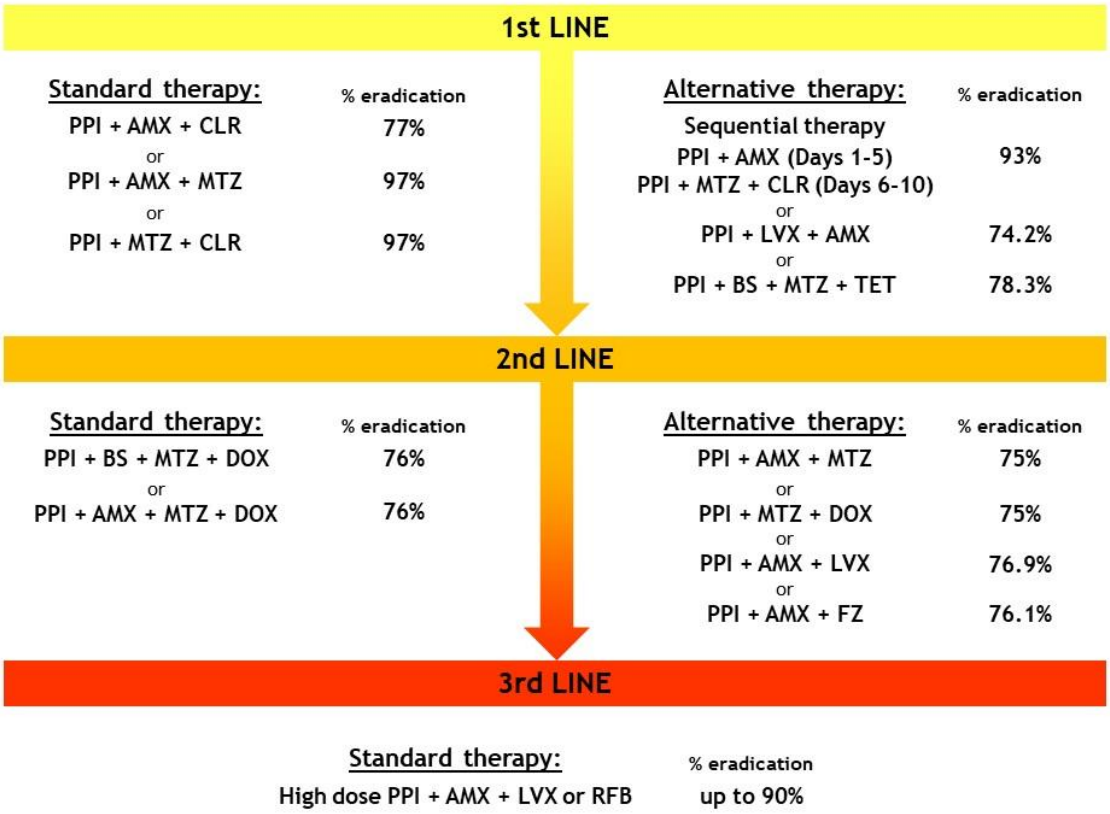

Figure 1.7 - Most common therapies for the treatment of *H. pylori* infection and respective eradication rates. Therapy selection should consider antibiotic resistance, patient allergies and drug availability. Abbreviations: proton pump inhibitor (PPI), amoxicillin (AMX), clarithromycin (CLR), metronidazole (MTZ), levofloxacin (LVX), bismuth salts (BS), tetracycline (TET), doxycycline (DOX), furazolidone (FZ), moxifloxacin (MXF) and rifabutin (RFB). Adapted from Table 2 in (45).

Antibiotic resistance is a global health threat associated with high morbidity and mortality. The overuse and misuse of antibiotics in human health and other sectors such as agriculture, together with the incorrect disposal of these compounds into the environment, has led to an insurgence of multidrug-resistant bacteria (51). The speed at which bacteria are acquiring resistance mechanisms and their complexity makes it so that the development of new antibiotics or alternative therapies cannot keep pace with them (51, 52). In 2017 *H. pylori* was classified by the World Health Organization as high priority in a list of 12 bacteria for which new treatment is urgently needed (53).

Poor patient compliance is yet another factor involved in treatment failure. Therapeutic regimens are complex, involving several dosages taken twice daily (or four times daily in the case of bismuth quadruple therapy) during a period of 7 to 14 days. Moreover, in the case of sequential therapy, it might involve switching antibiotics in the middle of this period (54). Together with the associated side-effects (abdominal pain, headaches, nausea, vomiting, diarrhea) that ail a significant number of individuals, this can contribute to patients stopping the treatment or taking it incorrectly, leading to lower eradication rates and further boosting antibiotic resistance (55).

In addition to these side-effects, the use of antibiotics is known to induce a dysbiotic state in the gut microbiota. The gut microbiota refers to the microorganisms that inhabit the gastrointestinal tract, where they have developed a complex and mutually beneficial relationship with the host (56). It is considered an essential factor in the balance between the health and disease of an individual, with advantages such as maintaining the integrity of the mucosal barrier, supplying the host with nutrients and vitamins, protection against pathogens and regulating the host's immune

system (56, 57). Exposure to antibiotics can alter the composition of the microbiota, reducing or impairing the mutualistic microbes and increasing susceptibility to infections from newly acquired pathogens or opportunistic bacteria already present and now able to overgrow. Also, these alterations can remain for a long time, from months to years, and the microbiome never fully reverts to its original state (58). The use of antibiotics, which are not specific for *H. pylori*, induce the impairment of the gut microbiota, leading to an undesirable state of antibiotic-driven dysbiosis (57, 59).

Finally, the presence of *H. pylori* biofilms in the stomach of infected patients is yet another factor influencing treatment outcome (60, 61). Biofilm formation is a strategy used by bacteria not only as a way of increasing protection against the harsh environment found in the stomach and antimicrobials, but it also helps with the evasion of the immune system and allows for higher genetic diversity due to enhanced recombination (62). Furthermore, the presence of biofilm is suggested to be associated with infection reoccurrence (63). The formation of these structures and their pathogenicity will be further detailed in the next subsection.

1.2. Biofilms

In general, a bacterial biofilm is defined as a group of bacteria, from the same or different species, adhered to a surface, biotic or abiotic, encased by an extracellular matrix made up of secreted polymeric substances (proteins, polysaccharides and extracellular DNA) (64, 65).

In the environment, bacteria form biofilms that protect them from antibacterial chemicals, environmental bacteriophages and phagocytic amoebae. In the human body, biofilms boost resistance to antibiotic therapy and the host clearance mechanisms (antibodies and phagocytes), contributing to their pathogenicity and leading to chronic biofilm infections (64, 66).

For eradication to be achieved, the compound must reach all the bacteria. This is not the case of many strategies since most are effective against planktonic bacteria but ineffective against biofilm bacteria. Mostly, this occurs because the antimicrobial agent cannot penetrate the full length of the matrix and diffuses much slower. This alters the rate of action of the antimicrobial and might also alter the antimicrobial itself through reactions with the components of the matrix (66, 67). Besides the polymeric matrix, biofilms are defined by altered growth rates and different gene transcription than the ones on planktonic cells. Slow growing bacteria are present in biofilms and their reduced metabolism leads to slower uptake of antimicrobials, reducing their efficacy (66).

In terms of clearance mechanisms, bacteria in the biofilm release antigens and stimulate the host immune system to produce antibodies. However, these are unable to reach and kill the bacteria within the biofilm and can instead end up damaging the surrounding tissues (67).

The formation of a biofilm is an ability of many bacteria (e.g. *Pseudomonas aeruginosa*, *Staphylococcus aureus, H. pylori*) and requires a series of steps as shown in **Figure 1.8**.

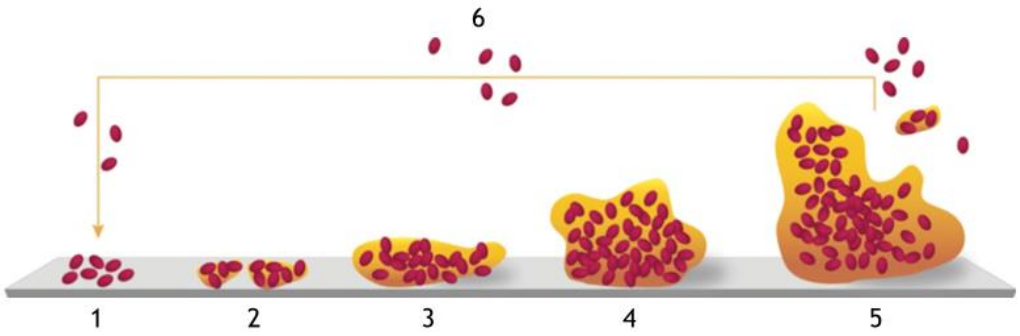

Figure 1.8 - Steps in biofilm formation. Sequentially, (1) attachment to a surface, (2) cell-cell aggregation, (3,4) growth and maturation, (5) detachment and (6) dispersion. Adapted from (68).

Generally speaking, biofilm formation begins with the non-specific attachment of bacteria to a surface through hydrophobic or electrostatic interactions, together with specific adhesion molecules in the bacteria's surface (**Figure 1.8 - (1)**) (69). This step is followed by the organization of bacteria in a monolayer and production of the extracellular matrix, leading to the formation of a multi-layered microcolony (**Figure 1.8 - (2) and (3)**) (69). Inside the biofilm, the bacteria adapt to the lack of oxygen and nutrients by suffering changes in metabolism, gene expression, protein production and cell division (**Figure 1.8 - (4)**) (64). Biofilms consist of both viable and dead bacteria, but are mostly composed of extracellular matrix, up to 90% of the biofilm biomass. This matrix is highly complex and variable, depending on the surrounding environment and the bacteria producing it. It is responsible for the mechanical stability of the biofilm, protection against adverse chemical and biological influences (osmotic stress, pH changes, antibiotics, the host immune system, grazing protozoa) and facilitates the exchange of genetic material and communication between bacteria (70). After bacterial and matrix growth, the biofilm reaches a maturation stage where it forms mushroom/tower-like structures (69). Dissolution of part of the matrix and the release of planktonic bacteria is the final step in this process and allows for spreading of the infection to other locations (**Figure 1.8 - (5) and (6)**) (69).

1.2.1. *Helicobacter pylori* biofilms

For *H. pylori, the* biofilm formation works as a virulence mechanism to increase its longevity in hostile conditions, such as the ones found in the environment and on the human body (e.g. nutrient depletion, oxygen levels, temperature, pH). These biofilms can be responsible for infection persistence even after several rounds of treatment (65).

In vitro, unlike most bacteria, *H. pylori* forms biofilm structures at the air-liquid interface (**Figure 1.9**). When bacteria attach to the walls of a glass tube or a glass coverslip, this is designated as an attached biofilm. Meanwhile, when bacteria form aggregates within an extracellular matrix but without attachment to a surface, as when grown in polystyrene well plates, it is often designated as a floating biofilm or a pellicle (71-73).

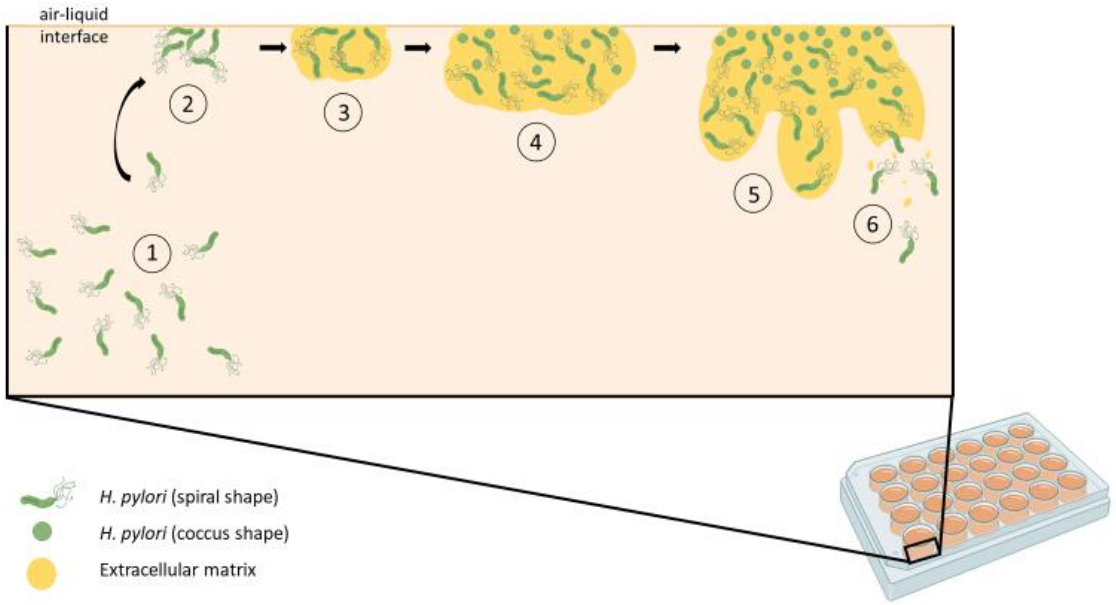

Figure 1.9 - Floating biofilm formation by *H. pylori* in a 24-well tissue culture flat-bottom polystyrene plate. (1) Free-swimming bacteria (planktonic state) move to the air-liquid interface and (2) become attached to each other by cell-cell interactions. (3) The bacteria start producing an extracellular matrix and multiplying, leading to (4) the formation of a microcolony. Further growth leads to a (5) mature biofilm when (6) dissolution of part of the matrix eventually occurs and allows the detachment of planktonic bacteria, that can then start colonization elsewhere.

H. pylori strains present differences in their ability to form biofilms. For instance, the *H. pylori* TK1402 strain is able to produce large amounts of biofilm biomass, while the SS1 strain generates much less (74). The morphology of the bacteria also diverges between these strains, with predominant bacillar conformation found in *H. pylori* TK1402 biofilms, while in the SS1 biofilms there are mainly coccoid bacteria (75, 76). Also, the differences in biofilm formation found among different studies might be justified by the use of different media or medium supllements, as well as different surfaces/substrates (62).

1.2.1.1. Composition

H. pylori biofilms are mainly composed of carbohydrates, proteins and extracellular DNA and can contain structures such as outer membrane vesicles (76). Each component will be briefly described.

Carbohydrates

Similarly to other biofilms, monosaccharides such as glucose, fucose and galactose are present in the *H. pylori* biofilm extracellular polymeric substance (EPS), showing a time-dependent increase in concentration, as well as N-acetylglucosamine and N-acetylmuramic acid (77-79). However, the main carbohydrate found in a mature *H. pylori* biofilm matrix is mannose in mannose-related proteoglycans (proteomannans) (77). All of these substances can also be found in *H. pylori*'s LPS (78).

Proteins

H. pylori forms a biofilm under conditions of poor nutrient availability and harsh environments and, as a consequence, many stress-induced proteins are upregulated. In mature biofilms, the total urease activity increases in a time-dependent manner and is higher than in planktonic bacteria. Other proteins can also be found, such as 60-kDa chaperonin, peroxiredoxin, catalase, citrate synthase, lipase, ferritin, glutamyl endopeptidase and neutrophil-activating protein A (NapA) (77).

Mutants for some of these proteins have been created to evaluate their significance in biofilm formation. For instance, the *napA* mutant showed a reduced ability to adhere to other bacteria and the substrate, altering microcolony formation and creating a biofilm with a looser structure (less compact than *H. pylori* wildtype) (77).

Extracellular DNA

Extracellular DNA (eDNA) plays an important role in the structure of many biofilms. However, in *H. pylori* biofilms, the degradation of this eDNA by DNase I, in a forming or mature biofilm, has little to no effect, showing that it might be less relevant for this bacterium (80).

It is hypothesized that the presence of eDNA allows for the exchange of genetic material, leading to transformation and promoting recombination events. Its origin is thought to be from cell lysis or secretion by transport vesicles. Further analysis has shown substantial differences between the eDNA and intracellular DNA, supporting the hypothesis that there is an active secretion of bacterial DNA through membrane vesicles and not only through cell lysis (80).

Studies have shown that both planktonic and biofilm bacteria have eDNA associated with outer membrane vesicles (OMVs) (76). These OMVs are nanosized structures made of bilayers of proteolipids derived from the outer membrane of Gram-negative bacteria. *H. pylori* OMVs have been shown to contain macromolecules such as urease, the adhesion proteins BabA and SabA and the cytotoxins CagA and VacA. They are associated with strong biofilm formation and thought to be involved in the attachment between cells, DNA transfers and the modulation of the immune system (75, 81).

1.2.1.2. Pathogenicity

As previously mentioned in section **1.1.1.,** the main routes for *H. pylori* infection transmission are thought to be environmental contaminations, with molecular studies detecting it in aquatic environments, such as water distribution systems, and person-to-person, with different reservoirs in the human body such as the dental plaque and the stomach. The presence of *H. pylori* biofilms in these different settings influences the bacteria's pathogenicity by increasing the risk of (re)-infection or its persistence (82, 83).

H. pylori biofilms in the environment

Dissemination of viable bacteria can happen through fecal material and can contaminate water sources used for human consumption, turning them into a source of infection (82).

Initial studies have focused on the presence of planktonic bacteria in drinking water. However, rather than associated with the water, *H. pylori* is mostly found in biofilms associated with the surface of pipes in water systems (82). Conventional culture techniques were incapable of detecting this bacterium mainly due to its ability to convert into a viable but non-culturable (VBNC) state as a defense from environmental stressors. Nonetheless, through molecular analysis techniques, such as polymerase chain reaction (PCR), *H. pylori* was identified in drinking water biofilms in both developed and developing countries (84, 85).

Mackay *et al.* initially investigated the presence of *H. pylori* in a mixed-species heterotrophic biofilm, similar to the ones found in water distribution networks and its persistence. This study showed that *H. pylori*, when in viable conditions, can be detected in the biofilm material by polymerase chain reaction (PCR) for up to 8 days (86). Recently, another study has confirmed this through additional techniques, such as peptide nucleic acid fluorescence *in situ* hybridization (PNA-FISH), increasing detection accuracy (87).

The analysis of distribution pipes removed from home water systems has confirmed the presence of these bacteria outside of laboratory reproductions (85). Additionally, they have shown their resistance towards standard water disinfection treatments since this bacterium is resistant to low concentrations of free chlorine that might kill other pathogens in biofilms (88, 89).

Through the use of contaminated water, it is also likely that food becomes contaminated. Some foods can provide *H. pylori* with the conditions needed for its survival, for example, raw vegetables. Different bacterial strains also differ in their ability to form a biofilm on the surface of vegetables, as this process depends both on the strain and the vegetable (90).

H. pylori biofilms in the human body

The stomach is a confirmed reservoir for *H. pylori* and the first evidence of biofilm formation in the gastric mucosa was acquired by Coticchia and Carron *et al*. by comparing gastric biopsies of urease-positive (*H. pylori* infection marker) and negative patients using scanning electron microscopy (SEM). Results showed that up to 97.3% of the surface area of urease-positive biopsy samples can be covered by a dense mature *H. pylori* biofilm, while urease-negative biopsy samples showed no biofilm (**Figure 1.10**) (60, 61).

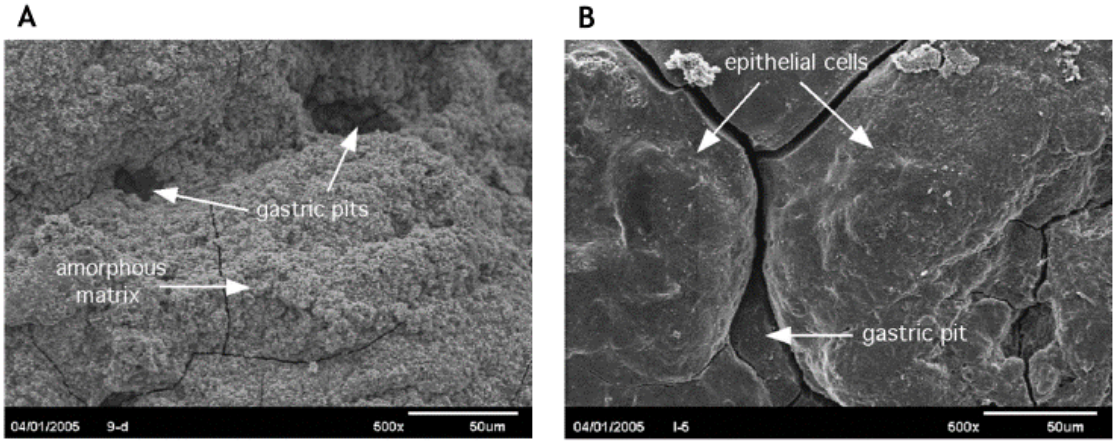

Figure 1.10 -SEM images of (A) the surface of the gastric mucosa covered in biofilm before treatment and (B) biofilm disappearance after *H. pylori* eradication. In (61).

Further research using SEM has detected the presence of *H. pylori* biofilms in the stomach of patients that underwent antibiotic therapy and suffered from a resurgence of the infection. This brings to light gaps in the eradication treatments, since biofilm formation is often overlooked (63).

Young et al. have proposed the transmission of *H. pylori* from the stomach to the oral cavity by reflux or vomiting, since viable bacteria have been found in the gastric juice of urease-positive patients (91). Indeed, through techniques such as PCR and SEM, *H. pylori* has been detected on the dental plaque, a biofilm growing on the surfaces of teeth, and in saliva. Once again, the ability of *H. pylori* to convert to a VBNC coccoid form, makes it harder to detect by the traditional culture methods but does not diminish its infectiousness (92).

Moreover, it has been shown that *H. pylori* can be found in the oral cavity of patients that underwent successful antibiotic therapy, indicating that prevalence in the oral cavity and the stomach are independent (93). Taking this into account, it is possible to hypothesize that the oral cavity might serve as an *H. pylori* reservoir and account for gastric reinfection (83).

1.2.2. Biofilm characterization techniques

There are several techniques avaliable to evaluate different biofilm characteristics, from biomass to morphology, to the number of viable bacteria. These are important for confirmation of biofilm formation and to study the effects that certain conditions and/or substances may cause in the biofilm.

1.2.2.1. Crystal violet assay

The crystal violet (CV) assay is a widely used method for quantifying total biofilm biomass. CV, a triarylmethane dye, is used as a histological stain and is one of the primary components in Gram staining. It is both cell membrane permeable in Gram-positive and Gram-negative bacteria and non-specific, as it does not distinguish between matrix, living and dead cells, giving an overall quantification of the biofilm components (**Figure 1.11**). After solubilization, with 90% v/v ethanol or dimethyl sulfoxide (DMSO), CV can be quantified by measuring absorbance at 530-600 nm using an UV-Vis spectrometer. The use of the CV assay to quantify the biomass of biofilms grown in a microtiter plate is inexpensive, reproducible, easy to perform and allows for analysis of many samples simultaneously. However, it is an indirect quantification method, as it gives a general idea of total biomass, but does not distinguish between live or dead cells. Also, this assay can be influenced by many variables (e. g. incubation time and temperature), introducing some variability between results (94).

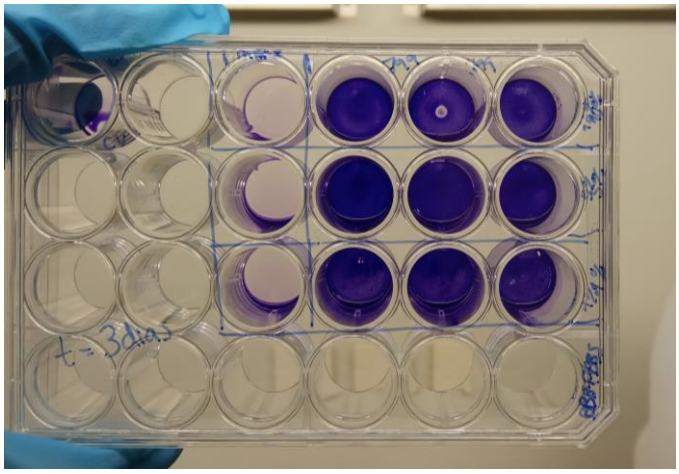

Figure 1.11 - Photograph of *H. pylori* J99 biofilms in 24-well tissue culture flat-bottom plate stained with CV.

1.2.2.2. Colony-forming units counting

Viable cell enumeration by plate count is a commonly used standard quantification method based on the concept that individual viable bacteria grow into colonies when plated on an agar plate (94). This allows for the quantification of live viable cells without the use of dyes. It can start with a liquid planktonic culture or, in the case of biofilms, these can be homogenized in a liquid medium or a buffer solution. Aliquots from this non-diluted sample are collected and serially diluted, for example in a microtiter plate, followed by plating in the proper agar plates where CFUs can be counted after incubation (**Figure 1.12**) (94).

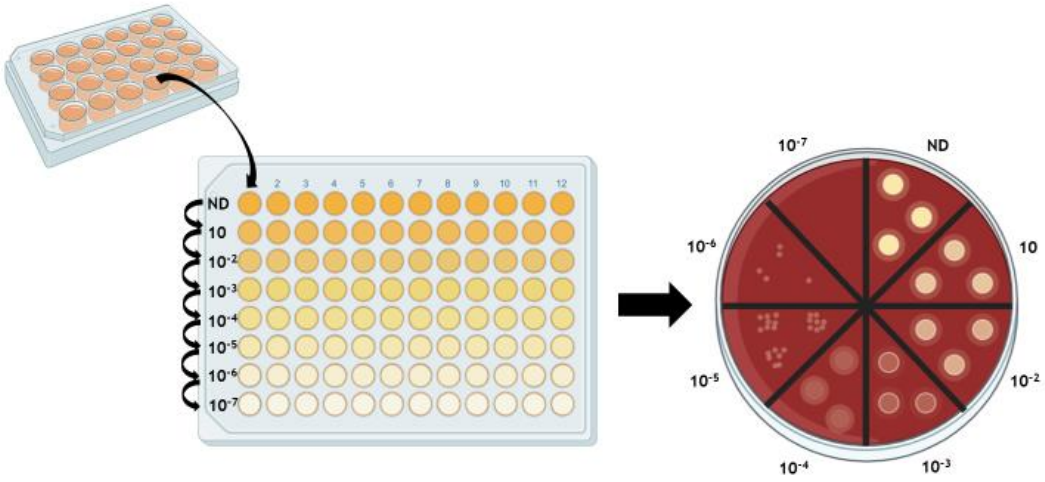

Figure 1.12 - Serial 10-fold dilution for CFU counting. ND – non-diluted.

The number of bacteria per milliliter (CFUs/mL) in the initial culture can then be calculated using **Equation 1.1**.

$$\frac{CFU}{mL} = \frac{CFU * 10^{n}}{V} \quad , \qquad \textbf{(1.1)}$$

where 10^{n} is the dilution factor and V is the plated volume.

It is important to mention that this technique only quantifies viable bacteria that are capable of forming colonies and not all of the viable bacteria in the sample (94).

Besides this limitation, this method is subject to contaminations and can be very time-consuming if the microorganism being studied is of fastidious growth. In the context of biofilms, it gives no information about the matrix and aggregates from insufficient biofilm homogenization can lead to errors. However, it does not require specialized equipment and can be performed for most microorganisms and from different types of sample origins (e. g. environmental, clinical) (94).

1.2.2.3. Scanning electron microscopy

Scanning electron microscopy (SEM) is a form of microscopy that gives information related to a sample's surface topography and composition (95). Unlike optical microscopes, which use light, the SEM uses a high-energy electron beam to scan the surface of a sample. As a result of the smaller wavelength, this system is able to resolve smaller features, under 1 nm in dimension. When it interacts with the sample, the electron beam causes the emission of secondary electrons and X-rays with an unique energy, which is detected and used to produce an image and to determine the sample's composition (95).

As shown in **Figure 1.13**, the SEM consists of an electron gun where the electron beam is generated, a column with a series of electromagnetic lenses to focus and reduce the diameter of the beam and a scanning coil to direct the beam in scanning the sample and, finally, the sample chamber. All of these components are under vacuum to allow the electron beam to form and reach the sample. These are connected to a detector and a computer system (96).

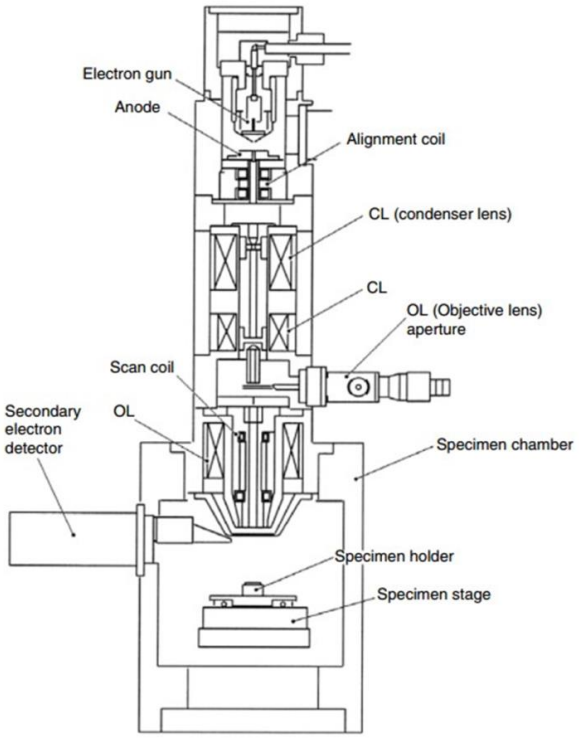

Figure 1.13 – Schematic diagram of a SEM. In (97).

In biofilm analysis, SEM provides high-resolution images and information such as the size and morphology of bacteria and the presence of EPS. This technique requires a pre-treatment of samples that involves gradual dehydration so they can withstand exposure to a vacuum. One disadvantage is that the dehydration process can lead to sample distortion and artifacts, especially in structures such as the EPS, which has a high water content. A way to mitigate this is by adding a fixation step with glutaraldehyde before dehydration, as this fixative helps to preserve the cell's structure (96). Another important step in sample preparation, for non-conductive samples, is a coating with a conductive material, such as gold, increasing conductivity and preventing charge buildup from the electron beam (96).

Overall, this technique provides high-quality images in a large range of magnifications and can give a variety of information, from topography to elemental analysis. However, analysis cannot be performed on live samples and it requires a preparation that might alter the sample (94).

1.2.2.4. Confocal laser scanning microscopy

Confocal laser scanning microscopy (CLSM) is a versatile form of microscopy that generates high-resolution complex three-dimensional images. The fact that a pre-treatment is not a requirement leads to a truer observation of samples and biofilms can remain fully hydrated, maintaining most of its characteristics. It allows for image processing and analysis, so the user can determine a variety of information such as the number of cells, dimensions, as well as reconstructing 3D structures (98).

In a widefield fluorescence microscope, the whole sample is evenly exposed to light and as such all areas are excited at the same time. This leads to some fluorescence detection outside of the focus field. The thicker the sample, the more the out-of-focus fluorescence signal interferes with image quality (99). On the other hand, CLSM focuses a laser through pinholes to excite the fluorophores of only a thin plane of the sample while rejecting out-of-focus light (100). To do so, the CLSM combines the fluorescence microscope hardware with a laser light source, specialized scanning equipment and digital imaging (**Figure 1.14**).

Figure 1.14 – Leica® TCS SP5 microscope setup (right) and schematic illustrating the principle of CLSM (left). PMT – photomultiplier tube. Adapted from www.leica-microsystems.com and (101).

As illustrated in **Figure 1.14**, the CLSM works by scanning the sample with a laser beam, using oscillating mirrors, and another system of mirrors and beam splitters to direct the return signal to the photomultiplier tube. The pinholes present in the light path select the fluorescence signals that come from the focused plane. Imaging of successive two-dimensional slices can be processed to create a three-dimensional image. The use of different lasers grants the ability to view multiple markers simultaneously (98).

Despite the above-mentioned advantages, this technique has some limitations, mainly the cost of the equipment compared to other microscopes and the limited depth (approximately 200 nm) (102).

1.2.3. Inhibition and eradication strategies

Due to their bactericidal properties against *H. pylori*, several compounds have been tested *in vitro* against its biofilm.

Pattiyathanee *et al.* proved that curcumin, a phytochemical found in turmeric, was able to inhibit the bacteria's ability to form a biofilm, although only for a limited time, as well as prevent their adhesion to the epithelial cells (103). Another compound tested was N-acetylcysteine (NAC), a mucolytic agent that can destroy the biofilm, leaving the bacteria more vulnerable to antibiotics. *In vitro* testing by Cammarota *et al.* has shown that in the presence of NAC (2 mg/mL), *H. pylori* is unable to form a biofilm and mature biofilms can be dissolved. In a clinical trial, when NAC was administered as a pre-treatment followed by an antibiotic course, it led to eradication rates of 65% for the treated group, much higher than the 20% achieved for the non-treated group (104). Overall, it is thought that a biofilm destabilization agent followed by or together with a bactericidal agent could be a good strategy to improve biofilm eradication (84).

Delivery systems have also been tested against *H. pylori* biofilms, namely lipid polymeric nanoparticles. In a study by Cai *et al.* lipid polymer nanoparticles were developed and tested against a *H. pylori* biofilm model. They were designed with an inner core of amoxicillin (AMX) and pectin sulphate and an outer layer containing a mixture of rhamnolipids and phospholipids. These nanoparticles were able to significantly disrupt the *H. pylori* biofilm, by fusion of the rhamnolipids with the extracellular polymeric substance (EPS), reducing the resistance of the biofilm to amoxicillin. At the same time, they were able to inhibit the adherence and colonization of *H. pylori* to target cells (105). Similarly, Li *et al.* developed clarithromycin loaded PEGylated lipid polymeric nanoparticles with a chitosan core and varying amounts of rhamnolipids. These nanoparticles were

able to penetrate the mucus and eradicate the *H. pylori* biofilm, showing enhanced eradication potential when compared to free clarithromycin (106).

However, the anti-biofilm effect of other vehicles for drug delivery, such as nanostructured lipid carriers (NLC), has yet to be explored. NLC will be discussed in more detail in section **1.3.**.

1.3. Nanostructured Lipid Carriers

Nanoparticles are materials with a size in the nanometer (10^{-9} m) range. Their small dimensions and high surface area provide them with unique physical and chemical properties and lead to applications in biology, medicine, pharmaceutics, electronics, etc. (107). Depending on their size, composition and shape they can be put into different classes such as dendrimers, quantum dots, carbon/metal/ceramic/polymeric/lipid nanoparticles, among others (107).

In the medical and pharmaceutical fields, nanoparticles can have many uses, being drug delivery the most common. An increase in the therapeutic effect and controlled release are some of the key advantages of using nanoparticles as drug delivery systems. Also, the fact that these materials are easy to manipulate allows their adjustment to different administration routes and targets, contributing to their acceptance (108).

Lipid nanoparticles are a class of nanoparticles that have become a popular drug delivery system for the oral delivery of both lipophilic and hydrophilic drugs. Their attractiveness comes from advantages such as the simple manufacturing techniques, easy scale-up and the controlled release of substances, contributing to increasing their bioavailability. Also, the use of affordable, easily available constituents, namely lipids listed as “generally recognized as safe” (GRAS) by the FDA, which can be metabolized by physiological metabolic pathways, increases their safety in comparison to polymeric nanoparticles (109).

Solid lipid nanoparticles (SLN), also called first-generation lipid nanoparticles, arise as a combination of the main advantages of liposomes and polymeric nanoparticles. Similarly to liposomes, they are composed of biocompatible materials and, like polymeric nanoparticles, their solid matrix protects the encapsulated drug from degradation and is susceptible to modifications to control release (110). They are formulated with solid lipids and offer the above-mentioned advantages. However, they possess a low loading efficiency and suffer drug expulsion during storage. This occurs due to their densely packed crystal network, which limits drug incorporation (110).

To overcome this disadvantage, nanostructured lipid carriers (NLC) were developed as a second-generation lipid nanoparticle. These are formulated with a blend of solid and liquid lipids, which create a structural organization with more imperfections that allow the incorporation of higher drug amounts. NLC have all of the advantages of the SLN, including their solid-state at body and room temperature, with the advantage of better loading efficiency and drug immobilization during storage (109, 110).

Depending on the selected drug, the selected lipids and surfactant and their concentration, the drug’s solubility and the production process, NLC can belong to one of three types (**Figure 1.15**).

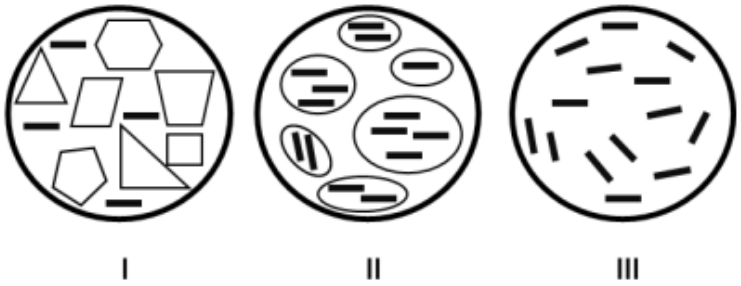

Figure 1.15 - Types of NLC: (I) Imperfect, (II) Multiple type and (III) Amorphous. Adapted from (111).

Imperfect type NLC (**Figure 1.15 - I**) are composed of small amounts of liquid lipid added to solid lipids. The structural and spatial differences of these lipids generate voids in the matrix, creating spaces for the drug to be contained. Multiple type NLC (**Figure 1.15 - II**) are obtained by mixing higher amounts of liquid lipid with the solid lipid, going beyond the solubility limit and causing phase separation. This creates nano-compartments in the solid matrix where lipophilic drugs can locate due to their higher solubility in the liquid lipid. Finally, amorphous type NLC (**Figure 1.15 - III**) can be obtained by mixing specific lipids (for example hydroxyoctacosanylhydroxystearate, isopropylmyristate or medium chain triglycerides, such as Miglyol® 812) that do not recrystallize after homogenization and cooling. This amorphous structure prevents drug expulsion through crystallization, improving stability during storage (110-113).

Due to their many advantages, NLC were selected in this work and they will be further explored in the following sections.

1.3.1. Production

There are different methods used to produce NLC. In general, these methods have a high yield and share a strong potential for scaling up to industrial production. Some of the most common NLC production techniques will be briefly highlighted.

High-pressure homogenization (HPC)

This technique can be performed at high temperatures (hot HPC) or temperatures below room temperature (cold HPC). In both cases, the drug is dissolved in the melted lipids at 5-10 °C above the melting point. For hot HPC, this mixture is blended with a heated aqueous surfactant solution and the high-speed stirring forms an emulsion with micro-sized droplets. To obtain nanoparticles this emulsion goes through a high-pressure (100-1500 bar) homogenizer multiple times and is then cooled at room temperature. For cold HPC, the emulsion is cooled using liquid nitrogen or dry ice and the microparticles formed are suspended in a cold aqueous surfactant and homogenized to form nanoparticles.

The use of cold HPC is better for the incorporation of hydrophilic drugs because it avoids the displacement of the drug from the nanoparticles to the aqueous phase by cooling and solidifying the particles before homogenization. Also, the brief use of high temperatures (only for melting the lipids) allows for the encapsulation of heat-sensitive drugs, without loss of their bioactivity (110, 112).

High shear homogenization and/or ultrasonication

This production method starts with the addition of the drug to the lipids that are melted at 5-10 °C above their melting point. Then, it is followed by the addition of a heated aqueous surfactant solution and the high-shear homogenization produces an emulsion. The following step is sonication,

which reduces the size of the droplets in the emulsion, producing nanoparticles after cooling at room temperature (110, 112).

Microemulsion

In this technique, a microemulsion is prepared by stirring together the lipids, which are melted at 5-10 °C above the melting point and a heated aqueous solution containing the surfactant. Then, dispersion is done in a high volume of cold water (2-3 °C) through stirring and the microemulsion breaks into nanoemulsion droplets that solidify into nanoparticles. The final dispersion is very diluted requiring an additional concentration step, with the added disadvantage of the high concentration of surfactants (110, 112, 114).

Solvent emulsification-evaporation

Unlike the previous methods, in the solvent emulsification evaporation method the lipid is dissolved in a water-immiscible organic solvent and then emulsified in an aqueous surfactant solution through constant stirring. During emulsification, the solvent evaporates, leading to lipid precipitation and forming nanoparticles. This method is good for the incorporation of heat-sensitive drugs since it can be fully conducted at room temperature. However, the use of organic solvents raises concerns about incomplete evaporation and the final dispersion is very diluted, due to the limited solubility of the lipid in the solvent (114).

Double emulsion

This technique is based on solvent emulsification-evaporation and is mainly used for loading hydrophilic drugs. First, the drug and the surfactant are suspended in an aqueous phase and are added to a mixture of melted lipids. Through mixing, this originates a primary water-lipid emulsion, which is then added and mixed with an aqueous solution to form a double emulsion (water-lipid-water). Surfactants are required to ensure that the drug does not transfer from the inner aqueous phase to the external water during solvent evaporation (110, 114).

Solvent diffusion

In this method, the lipid is dissolved in a water-miscible organic solvent. The organic solvents are saturated with water to ensure the initial thermodynamic equilibrium of both liquids and then the emulsion is added to water under constant stirring, leading to solidification and formation of the nanoparticles. This method presents the same disadvantages as solvent emulsion-evaporation, namely the use of organic solvents and over-dilution (114).

Solvent injection

Similar to solvent diffusion, the lipid is dissolved in a water-miscible organic solvent, but the mixture is rapidly injected through a needle into an aqueous solution of surfactants. The gradual diffusion of the solvent out of the lipid-solvent droplets causes a reduction in nanoparticle size and increases lipid concentration. Once again, the use of organic solvents is the main disadvantage of this method (110, 114).

1.3.2. Nanoparticle characterization techniques

1.3.2.1. Dynamic light scattering

Particles in a liquid suspension move under Brownian motions due to their interaction with the solvent. Dynamic light scattering (DLS) analysis is able to measure nanoparticle size by exposing

these particles to a light beam, which along with their movement leads to scattering in all directions as a function of the size and shape of the particles (**Figure 1.17**).

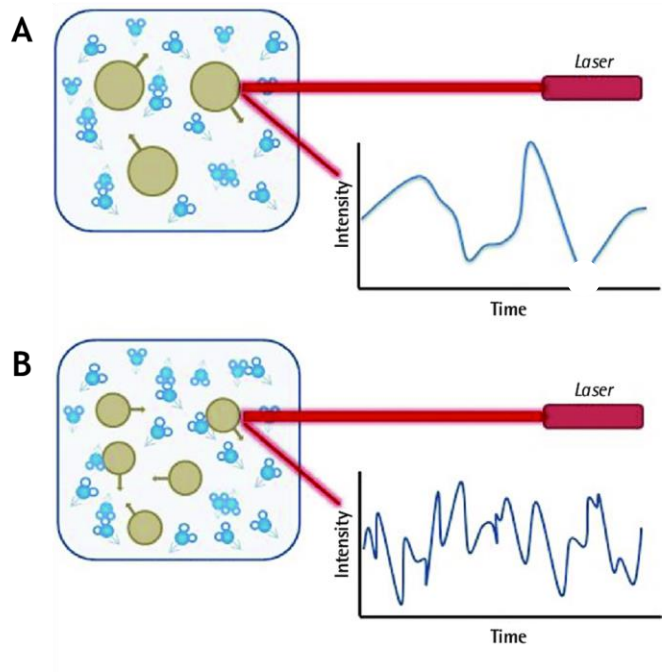

Figure 1.16 - Intensity changes in scattered light in dynamic light scattering from (A) large and (B) small particles. Adapted from (115).

Information regarding particle size can be obtained when monitoring the movement of particles over time through their scattered light since large particles diffuse slower than small particles. This scattered light is detected by the instrument and translated into the diffusion coefficient of the nanoparticles, which in turn allows for the determination of their size using the Stokes-Einstein formula (**Equation 1.2**):

$$D = \frac{K \cdot T}{6\pi \cdot \eta \cdot R} \quad , \tag{1.2}$$

where D is the diffusion coefficient, K is the Boltzmann coefficient, T is the absolute temperature and η is the viscosity of the medium (116).

DLS also provides information about the size distribution of the nanoparticles with the polydispersity index (PdI). The PdI ranges from 0 to 1 and a lower PdI represents a more monodisperse nanoparticle suspension. Although dependent on the type of nanoparticle, a PdI inferior to 0.3 is considered optimum by most researchers (117).

1.3.2.2. Electrophoretic light scattering

The zeta potential (ZP) can be defined as the potential difference between the particle and the surrounding medium measured in the shear plane, as shown in **Figure 1.18**.

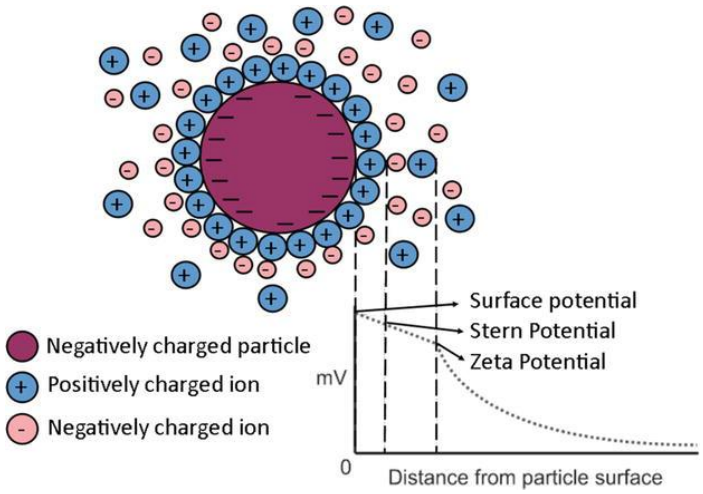

Figure 1.17 - Diagram illustrating the surface and zeta potential as a function of distance in a negatively charge particle. In (118).

ZP indicates the overall surface charge of the particles in a specific medium and can give information about its interaction with other molecules and the stability of the system. For instance, particles with high surface charge create electrostatic repulsion between particles with identical charges, stabilizing the suspension. On the opposite, low surface charges can lead to nanoparticle aggregation. It has been established that a ZP of approximately +30 or -30 mV provides a good stabilization of nanodispersions (114, 118).

Electrophoretic light scattering (ELS) analysis applies an external electric field to the sample leading to the movement of the nanoparticles according to their charge. Their velocity is then measured by the scattered light caused by the movement of the particles and can be converted into the zeta potential through Henry's function (**Equation 1.3**):

$$U_E = \frac{2\varepsilon z}{3\eta} f(ka) \ , \tag{1.3}$$

where U_E is the electrophoretic mobility, ε is the dielectric constant, z is the zeta potential, η is the viscosity and f(ka) is the Henry's function (119).

1.3.2.3. Nanoparticle tracking analysis

Nanoparticle tracking analysis (NTA) uses the properties of light scattering and the particles Brownian motion to obtain size distribution and the concentration of the particles in a liquid suspension. As opposed to DLS, NTA performs measurements on all the individual particles in the suspension, suffering less interference from particle aggregates or larger particles in a heterogeneous sample. A laser beam goes through the sample chamber and its light is scattered by the particles, this scattering is visualized in an optical microscope and recorded by a mounted camera. This camera is able to capture a video of the particles moving, which in turn is analyzed by software that tracks the individual particles and calculates their hydrodynamic diameters (120).

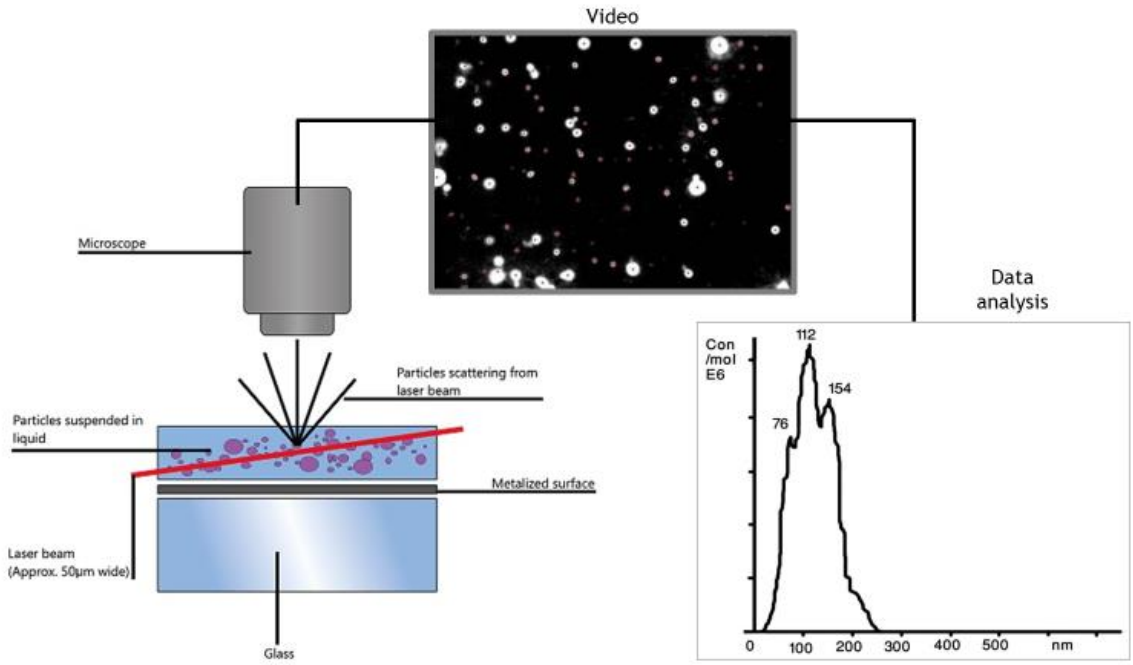

Figure 1.18 - Diagram of NTA main steps, light scattering detection, video recording and data analysis. Adapted from www.malvernpanalytical.com and (121).

1.3.3. Applications of NLC

NLC seem to be a promising strategy to be used both in therapeutics and in the cosmetic industry. In fact, the first marketed products containing NLC were two cosmetic creams: Nanobase® from the company Yamanouchi and Cutanova® from Dr. Rimpler GmbH (122). Although the study of lipid nanoparticles has resulted in an increasing number of applications and registered patents, most of the existing commercialized products containing NLC are cosmetics or licensed as "nutraceuticals", such as FloraGo® from Kemin Industries (123).

Due to the complexity of regulations concerning the application of a new therapy in the clinic, many patents remain in the initial stage and do not result in commercialized products. Cosmetic products have the advantage of higher economic investment and a faster process, since they do not require such strict clinical evaluation. Meanwhile, the exponential development of nanotechnology and nanomaterials has raised several ethical and safety concerns and resulting regulatory questions that increase the difficulty of the commercialization process (123, 124).

Nevertheless, many studies with NLC have shown their potential in various medical areas (**Figure 1.16**) (125-127):

- increasing the absorption of drugs (e. g. anesthetics, antifungals, growth factors) through dermal and transdermal routes of administration;
- increasing the bioavailability of lipophilic drugs (e. g. by protecting them of the gastric environment and penetrating the mucus barrier);
- in pulmonary delivery, NLC can transport drugs across the pulmonary endothelium and show reduced toxicity;
- they can penetrate the many ocular barriers and can be modified to prolong drug retention;
- in cancer treatment, through the targeted delivery of chemotherapeutics and tumor gene therapy using NLC to deliver microRNAs.

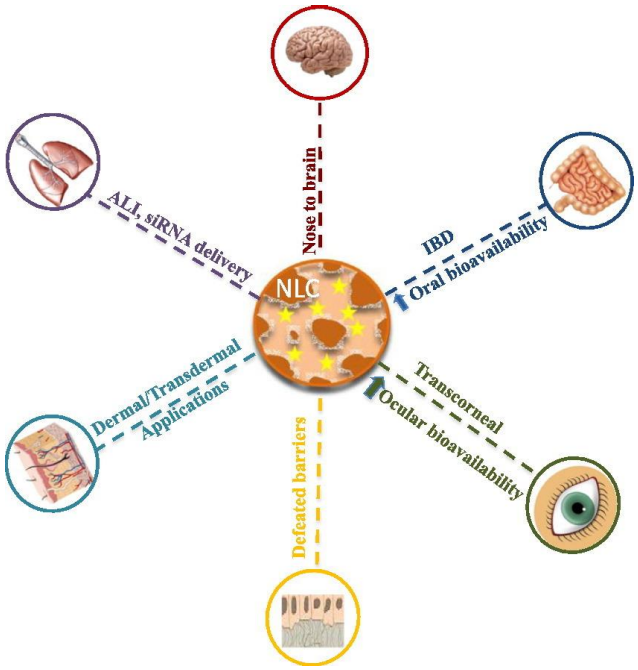

Figure 1.19 - Examples of NLC routes of administration and applications in medicine. ALI – air-liquid interface, IBD – inflammatory bowel disease. In (125).

Recently, nanosized drug delivery systems have become increasingly relevant for the delivery of antimicrobials. This is the case with the treatment of *H. pylori* infection, where nanoparticles for oral delivery, such as lipid and polymeric nanoparticles, have the ability to protect bioactive compounds from the harsh environment of the digestive tract and reach the pathogen through the mucus barrier (108, 128).

For example, substances such as docosahexaenoic acid (DHA), an omega-3 polyunsaturated fatty acid present in fish oil, have been proven as effective against *H. pylori* (129). However, DHA is easily oxidized leading to loss of its bioactivity. To overcome this challenge, Seabra *et al.* developed NLC loaded with DHA (DHA-NLC) produced by hot homogenization and ultrasonication using a blend of lipids and a surfactant. *In vitro* studies showed an enhanced DHA bactericidal effect when encapsulated in the NLCs (130).

Further studies demonstrated the ability of the NLC, even without DHA, to be bactericidal against *H. pylori* J99 strain at low concentrations, by destabilization of the bacteria's membrane and its disruption (131).

Moreover, considering that this gastric infection is characteristically multi-strain, it was important to evaluate the ability of the U-NLC and DHA-NLC to kill different *H. pylori* strains. Briefly, through *in vitro* testing, minimal inhibitory concentrations (MIC) and minimal bactericidal concentrations (MBC) were established for *H. pylori* 26695 (ATCC® 700392™) and *H. pylori* NCTC 11637 (ATCC® 43504™) strains and both NLC proved bactericidal at low concentrations. The nanoparticles safety towards bacteria from the normal and dysbiotic gut microbiota was also assessed due to the role that these microorganisms play in the overall health of an individual. The strains tested were *Lactobacillus casei*-01 and *Escherichia coli* ATCC® 25922™ (131), *Pseudomonas aeruginosa* ATCC® 27853™, *Staphylococcus aureus* ATCC® 33591™, *Escherichia coli* ATCC® 25922™, clinical isolates of *Enterococcus faecalis* and *Salmonella sp enteric, Bifidobacterium longum* CIP 64.62, *Bifidobacterium breve* NCIMB® 702258, *Bifidobacterium animalis* subsp. *lactis* BB-12®, *Bifidobacterium adolescentis* DSMZ® 20083 and *Lactobacillus acidophilus* LA-5® (**Appendices I and II**). Results showed that both types of nanoparticles, at the concentrations tested, did not interfere

with the gut microbiota, adding a huge advantage to this strategy over antibiotics (**Appendices I and II**).

Due to the potential of these NLC for the treatment of *H. pylori* infection and the recent information about this pathogen's ability to produce a biofilm, this work aimed to evaluate the effect of these NLC on mature *H. pylori* biofilms.

Chapter 2 – Materials and Methods

2.1. Nanostructured Lipid Carriers (NLC) production

Unloaded nanostructured lipid carriers (U-NLC) and nanostructured lipid carriers loaded with docosahexaenoic acid (DHA-NLC), were prepared following the protocol by Seabra *et al*. (130). Briefly, using previously sterilized material, 90 mg of the liquid lipid Miglyol® 812 (Acofarma, Spain), 200 mg of the solid lipid Precirol® ATO5 (Gattefosé, France) and 60 mg of the surfactant Tween® 60 (Merck, Germany) were weighted and then heated at 65 ºC in a water bath until the solid lipid melted. For the DHA-NLC, 84 µL of DHA (Cayman Chemical Company, USA) was added for a final concentration of 5 mg/mL. Then, 4.2 mL of heated type I water was added, followed by homogenization for 20 seconds using an ultra-turrax (T25 Janke and Kunkel IKA-Labortechnik, Germany) at a speed of 12000 revolutions per minute (rpm) and sonication (Vibra-Cell model VCX 130, equipped with a VC 18 probe, tip diameter of 6mm, Sonics and Materials Inc., Newtown, USA) for 5 minutes with an amplitude of 60%.

To evaluate the sterility, nanoparticles were plated in Trypticase Soy agar (TSA) plates and incubated at 37 ºC for 24h.

Nanoparticles were stored at 4 ºC, protected from light and for a maximum period of 2 weeks as described (130).

2.2. Nanostructured Lipid Carriers characterization

2.2.1. Size and zeta-potential

Size and surface charge of the NLC were determined using a Zetasizer Nano ZS (Malvern Instruments, UK). This equipment can perform Dynamic Light Scattering (DLS) and Electrophoretic Light Scattering (ELS) analysis to measure diameters and zeta potential (ZP), respectively.

NLC were diluted in a 1:50 ratio in type I water and placed in a disposable capillary cell. Measurements were taken at a backscattering angle of 173° and at a temperature of 37°C, as described by Seabra *et al*. (130).

2.2.2. Concentration

NLC concentration was analyzed using a NanoSight N300 (Malvern Instruments, UK), which uses the Nanoparticle Tracking Analysis (NTA) technology. Briefly, NLC concentration was adjusted to 1.25% v/v and then diluted in a 1:20000 ratio in type I water (130).

2.3. *H. pylori* biofilm production

2.3.1. *H. pylori* culture

H. pylori J99 (ATCC® 700824™) strain (provided by the Department of Medical Biochemistry and Biophysics, Umeå University, Sweden) was selected due to its ability to form biofilms (132, 133).

H. pylori was grown in solid medium plates composed of blood agar (Liofilchem, Italy) supplemented with 10% v/v defibrinated horse blood (TCS Biosciences, UK) and a 0.2% v/v antibiotics-cocktail (0.155 g/L polymyxin B, 6.25 g/L vancomycin, 1.25 g/L amphotericin B and 3.125 g/L trimethoprim; Sigma-Aldrich, USA). Initially, bacteria were grown by culturing in 20 µL spots for 48h, followed by spreads for 48h. Bacteria were incubated at 37 °C under a controlled microaerophilic environment (5% O_2, 15% CO_2, 80% N_2) created using a gas-generating pack (Campygen™; Thermo Fisher, USA) in a sealed jar. Afterward, bacteria were transferred to a liquid medium composed of Brucella broth (BB, Sigma-Aldrich, USA) supplemented with 10% v/v heat-inactivated fetal bovine serum (FBS; GIBCO, USA) and the bacterial concentration was adjusted to approximately 10^9 colony-forming units (CFUs)/mL (equivalent to an optical density (OD) of 0.1 at λ=600nm) (134). Then, this pre-inoculum was incubated overnight (20 hours) at 150 rpm and under the above-mentioned conditions of temperature and atmosphere.

2.3.2. *H. pylori* biofilm

The biofilm growth protocol was adapted from the one of Windham *et al*. (62). Briefly, 1 mL of *H. pylori* J99 inoculum (10^9 CFUs/mL) prepared in **2.3.1** was added to the wells of a 24-well tissue culture flat-bottom plate (Falcon®, USA).

The conditions to obtain a model of a mature biofilm were optimized by evaluating the percentage of FBS used to supplement the BB media (1% or 5% versus the usual 10% v/v), as well as the growth incubation time (2, 3 and 5 days). Plates were incubated under stirring at 100 rpm and at the same microaerophilic and temperature conditions above-mentioned. Every 48h, media was carefully removed from under the floating biofilm and gently replaced with fresh media without disturbing the biofilm. At the different time-points: 2, 3 and 5 days, the biofilms and planktonic bacteria were quantified as described in section **2.5**.

2.4. Effect of the NLC on *H. pylori* biofilms

To determine the effect of the NLC on the eradication of mature *H. pylori* biofilms, the latter were grown as described in **2.3.** and under conditions selected as optimal (BB supplemented with 5% FBS, 3 days). Afterwards, biofilms were incubated with 300 µL of U-NLC or DHA-NLC at different concentrations (0.156% up to 40% v/v). As a positive control, the biofilms were incubated only with 300 µL of liquid medium. The effect of water (the solvent used in NLC suspensions), was also evaluated by incubating the biofilms with 300 µL of liquid medium with a volume of water equivalent to the volume of NLC suspension added at the highest concentration tested (40% v/v). The biofilms were then incubated for 24h at 37 °C, in a microaerophilic environment, at 150 rpm.

NLC concentrations were expressed in percentage (%) volume of NLC suspension/total volume. For instance, the highest concentration tested, 40% v/v, corresponds to the dilution of 120 µL of NLC suspension in media for a total volume of 300 µL. The following concentrations up to 0.156% v/v were a result of a serial dilution in a 1:2 ratio. For the control with media and water, instead of 120 µL of NLC suspension, 120 µL of water was added.

2.5. *H. pylori* biofilm quantification

2.5.1. Biofilm biomass quantification

Biofilm biomass quantification was performed using a modified version of the protocol described by Yang *et al*. (77). Briefly, the media was carefully removed from under the floating biofilm and plates were centrifuged at 3000 *g* for 5 minutes. Then, the wells were rinsed three times with 1x phosphate-buffered saline (PBS, pH 7.4) and dried at 37 ºC for 10 minutes. Afterward, 300 µL of crystal violet (CV) (Sigma-Aldrich, USA) at 0.1% v/v was added to each well. A negative control was performed using a well with only culture media. Incubation proceeded for 5 minutes under stirring at 75 rpm and protected from light. The excess of crystal violet was removed and the wells were rinsed three times with PBS 1x. Finally, the CV was solubilized in 300 µL of dimethyl sulfoxide (DMSO 99% v/v; VWR, USA), samples were diluted in a 1:10 ratio in DMSO and absorbance was measured at 595 nm in the Synergy™ Mx Monochromator-Based Multi-Mode Microplate Reader (BioTek Instruments®, USA).

2.5.2. Bacteria viability evaluation

Bacterial viability was accessed by colony-forming units (CFUs) determination. CFUs were quantified in both planktonic bacteria and on the formed biofilms. For that, the liquid media containing planktonic bacteria was collected and then the biofilms were mechanically destroyed in 1 mL of PBS 1x (pH 7.4). Both planktonic and biofilm bacteria were serially diluted 10-fold in PBS 1x and plated in *H. pylori* solid medium as described in **2.3.1.,** in concentrations ranging from non-diluted to a dilution factor of 10^7. Plates were incubated at 37ºC, under microaerophilic conditions as mentioned in **2.3.**. After 4 days, CFUs were counted and the CFUs/mL were calculated using **Equation (1.1)**.

Confocal laser scanning microscopy (CLSM) was used for the imagining of the *H. pylori* biofilms and a Filmtracer™ LIVE/DEAD™ Biofilm Viability Kit (LL10316; Invitrogen™, USA) was used for the staining following the manufacturer's instructions. Briefly, biofilms were grown in a black 24-well µ-plate with flat coverslip bottom (Ibidi®, Germany), as described in section **2.3.,** and the NLC were added to biofilm as described in section **2.4**. As a positive control, the biofilms were incubated with 300 µL of liquid medium and, as a negative control, the biofilms were incubated with PBS 1x. The incubation with PBS 1x was chosen as a negative control since the complete depletion of nutrients induce bacterial death and, therefore, it was used to adjust the fluorescence intensity of propidium iodide (PI). After incubation, the growth media was carefully removed and the biofilms were washed with NaCl 0.9% v/v solution. Fixation of the biofilms allowed easier manipulation during the staining process and imaging and, when compared with non-fixed biofilms, no significant impact on viability was detected. As such, the biofilms were fixed by incubation with 300 µL of 4% v/v paraformaldehyde (PFA; Sigma-Aldrich, USA) for 30 minutes. PFA was removed and the biofilms were washed with NaCl 0.9% v/v. For the staining, 3 µL of SYTO 9 and 3 µL of PI was added per mL of type I water (0.22 µm filter-sterilized). SYTO 9 stains total bacteria, live and dead, while PI only stains bacteria with compromised membranes, dead or damaged bacteria. Then, 300 µL of this mixture was added to the biofilms and these were incubated for 30 minutes, protected from light. The stain was removed and the biofilms were washed with NaCl 0.9% v/v. To prevent drying, the stained biofilms were covered with 300 µL of NaCl 0.9% v/v. Biofilms were visualized using a Confocal Leica TCS SP5 (Leica Microsystems, Germany). The bacteria stained with SYTO 9 were examined with excitation at 488 nm and the bacteria stained with PI with excitation at 561 nm. The acquisition was obtained with an HCX PL APO CS 40.0x1.30 OIL UV objective and an HCX PL APO CS 63.0x1.40 OIL UV objective, and biofilm stacks were obtained with a step-size of 0.46 µm.

2.5.3. Morphology evaluation

Scanning electron microscopy (SEM) was used to evaluate the morphology of the *H. pylori* biofilms. Biofilms were grown as previously described in section **2.3.**, using 24-well plates with a sterile 12 mm glass coverslip (Marienfeld, Germany) on the bottom of each well. The NLC were added to the biofilm as described in section **2.4.**. As a positive control, the biofilms were incubated with 300 µL of liquid medium, and as a negative control, the biofilms were incubated with PBS 1x. The growth media was carefully removed and biofilms were washed with PBS 1x and fixed with 2.5% v/v glutaraldehyde (Sigma-Aldrich, USA) in 0.14 M sodium cacodylate buffer (Sigma-Aldrich, USA). After 30 minutes, the glutaraldehyde was removed and biofilms were washed with PBS. Biofilms were then dehydrated with a growing ethanol/water gradient (50, 60, 70, 80, 90, 99% v/v). Samples were kept overnight in ethanol 99% v/v (Merck, Germany), at 4 ºC, and then were submitted to the critical point dryer (CPD7501, Polaron Range) to remove the ethanol. Finally, samples were sputter-coated with a gold/palladium film over 30 seconds and bacterial morphology was visualized by SEM (JEOL JSM-6310F) at magnifications of 250x, 2500x and 10000x, at CEMUP (Centro de Materiais da Universidade do Porto).

2.6. Statistics

Statistical analysis was performed with Graph Pad Prism 8.0 (Graph-Pad Software, La Jolla, USA). Results are presented as the mean ± the standard deviation (SD). A p value of <0.05 was considered statistically significant.

Statistical significance was determined using the one-way ANOVA test (Tuckey's multiple comparisons test) for comparisons between the different conditions tested for nanoparticle optimization and between the different media tested for biofilm optimization. The one-way ANOVA test (Dunnett's multiple comparisons test) was used for comparisons of treated and untreated biofilms and the Mann-Whitney test for comparison between controls.

Chapter 3 – Results

3.1. Nanostructured Lipid Carriers

One of the first steps in nanoparticle production is the optimization of the production process. Although previously optimized as described by Seabra *et al*. (130, 131) and produced in the developed Project (**Appendices I and II**), it was important to evaluate how the sonication amplitude, sonication time and cooling method might influence the NLC. For that, U-NLC were used as a model and changes were measured in terms of size, surface charge by zeta potential (ZP) and polydispersity index (PdI) and are shown in **Figure 3.1**.

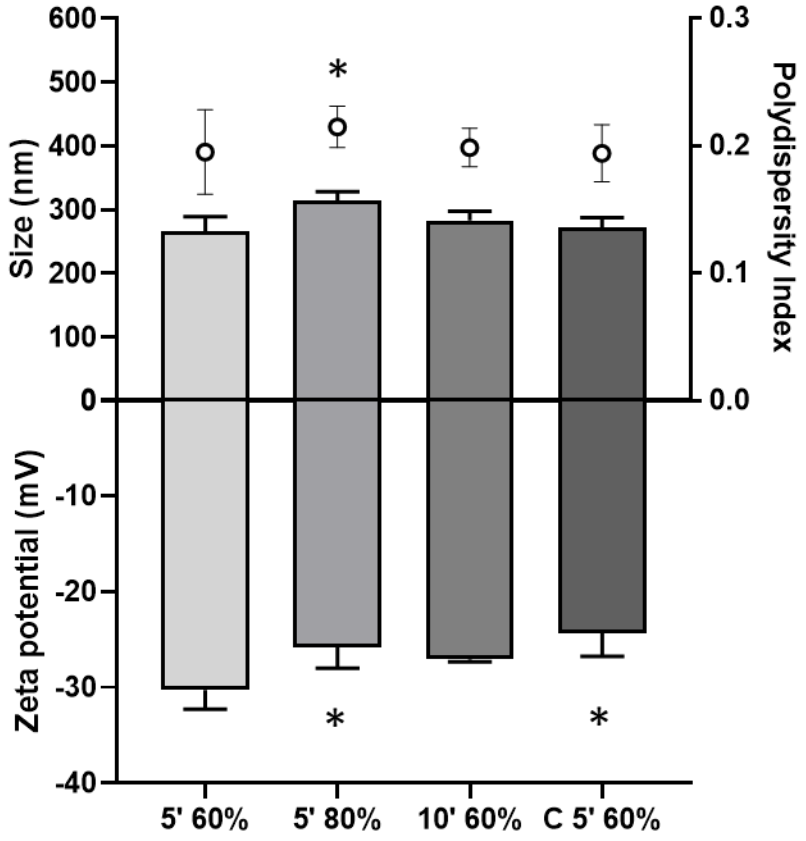

Figure 3.1 - Characterization of U-NLC. U-NLC were characterized in terms of size (positive bars), zeta potential (negative bars) and polydispersity index (PdI) (dots) using a Zetasizer Nano ZS. Measurements were taken at 37° C. The conditions tested are expressed in minutes (') and sonication amplitude in percentage (%). Controlled cooling (C) was also evaluated by cooling samples at 25 ºC, for 1 hour, at 150 rpm. Size and zeta potential: *p<0.05, statistically significant differences between alternative conditions and the previously established protocol (5' 60%). PdI: no statistically significant differences. n=3.

The production of the U-NLC was successful in all conditions tested. A sonication step with an amplitude of 60% for 5 minutes without controlled cooling was used as a control. The effect of sonication amplitude was evaluated by increasing it from 60% to 80% and resulted in an increase in diameter from approximately 267 nm to 314 nm and an increase in zeta potential from -30 mV to -26 mV. Regarding the sonication time, an extension from 5 to 10 minutes did not result in significant differences. The controlled cooling only impacted the U-NLC zeta potential, leading to an increase from -30 mV to -24 mV. The polydispersity index remained low, i.e. around 0.2, indicating that all conditions evaluated resulted in monodisperse and homogeneous size distribution.

The conditions used for NLC production (U-NLC and DHA-NLC) were a sonication amplitude of 60% for 5 minutes. Characterization is shown in **Figure 3.2**.

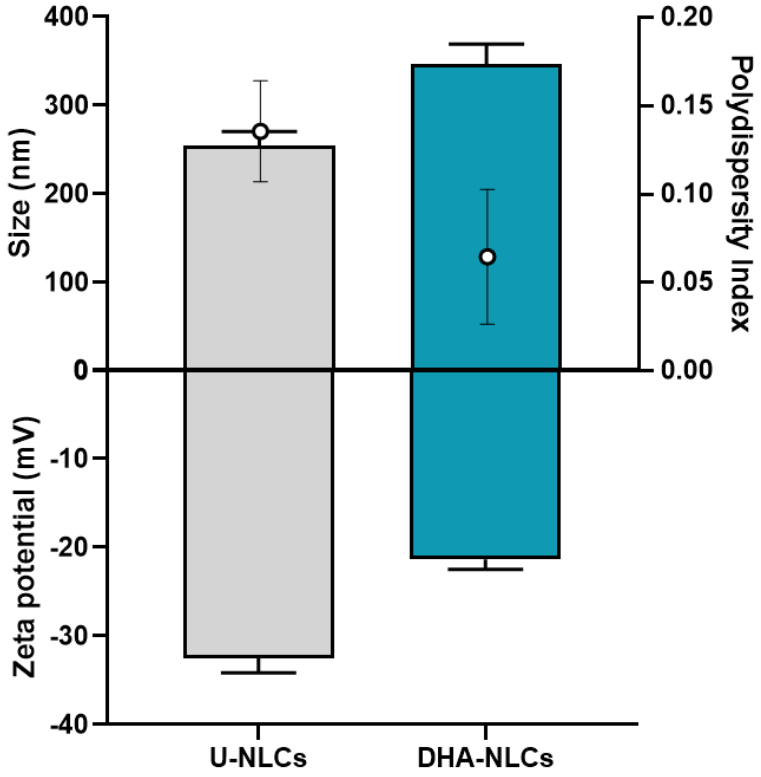

Figure 3.2 - Characterization of U-NLCs and DHA-NLCs. NLC were characterized in terms of size (positive bars), zeta potential (negative bars) and polydispersity index (PdI) (dots) using a Zetasizer Nano ZS. Measurements were taken at 37° C. n=4.

Both types of NLC were successfully produced and characterized. U-NLC presented a diameter of approximately 255±16 nm and a surface charge of -32±2 mV, while DHA-NLC presented a diameter of roughly 346±23 nm and a surface charge of -21±1 mV. NLC showed a homogeneous size distribution with low PdI for both types of formulations 0.14 and 0.06 for U-NLC and DHA-NLC respectively.

To determine the concentration of the nanoparticles, NTA was carried out. Two representative frames of the NTA videos are shown in **Figure 3.3** and the determined concentrations are presented in **Table 3.1**.

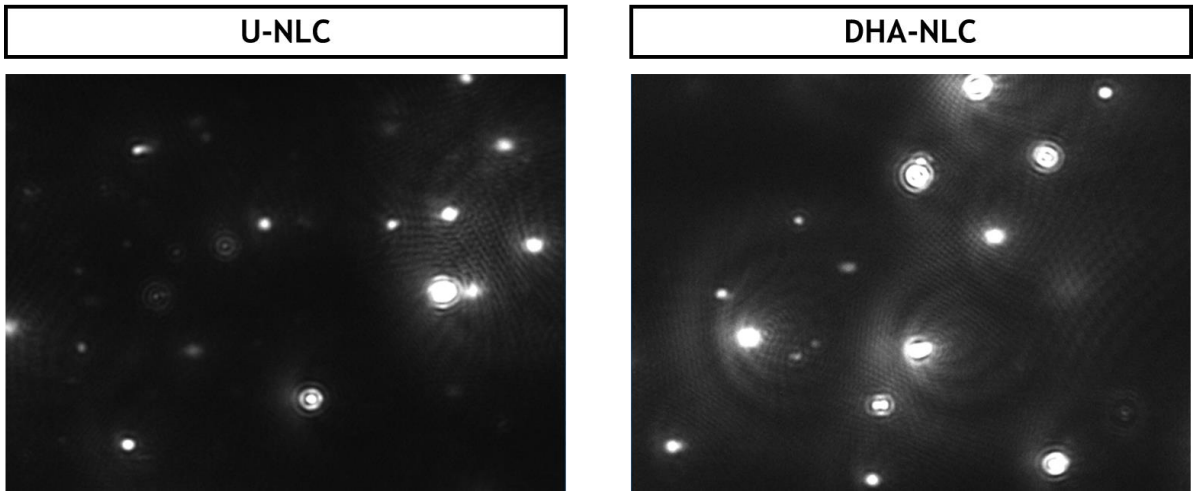

Figure 3.3 - Representative frames from the video produced for NTA by NanoSight N300. Images show the light diffracted by the NLC. By tracking the nanoparticle's movement NTA can determine their size.

The videos captured for the NTA show that the nanoparticles do not form aggregates, confirming their stability in the suspension.

Table 3.1 - Nanoparticle concentration of NLC determined by NTA using a NanoSight N300. Measurements were taken at RT. Results are presented as the mean ± the standard deviation (SD) and pertain to a 1.25 %v/v suspension of NLC.

U-NLC	DHA-NLC
$7.35 \times 10^{12} \pm 3.13 \times 10^{12}$ particles/mL	$4.49 \times 10^{12} \pm 6.34 \times 10^{11}$ particles/mL

In terms of concentration, the obtained results for U-NLC and DHA-NLC are similar and in the same order of magnitude (10^{12}) as previous results obtained by Seabra *et al.* (130).

3.2. *H. pylori* biofilms

The production of biofilms by *H. pylori* can be influenced by the nutrients available, which can be altered by simply changing the FBS supplement to the culture media (62, 135). As such, during the initial optimization of the biofilm model, the liquid medium was supplemented with varying concentrations of FBS: 1% or 5% and compared with the standard 10 %v/v used for optimal growth. Biofilm formation was evaluated by total biomass quantification using the CV assay (**Figure 3.4**) and the number of viable cells by CFU counting and calculation of CFUs/mL (**Figure 3.5**).

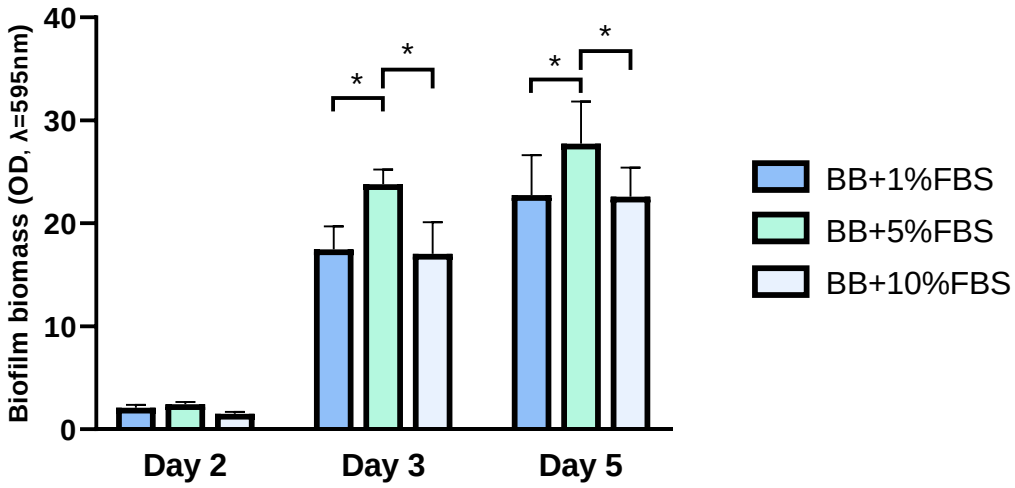

Figure 3.4 – Total biofilm biomass quantification using the CV assay (OD, λ= 595 nm). Biomass was quantified at 2, 3 and 5 days of biofilm growth. Biofilms were grown in liquid medium (Brucella broth, BB) with different concentrations of fetal bovine serum (FBS), 1%, 5% and 10% v/v. *p<0.05, statistically significant differences between biofilm biomass between conditions. n=3

After 2 days of growth, the biofilm shows only a reduced amount of biomass and no significant differences between conditions. Then, exponential biomass growth occurs during the next 24h (day 3) and it keeps increasing up to day 5 on all conditions (**Figure 3.4**). No statistically significant differences were seen between the use of BB+10% FBS and BB+1% FBS. However, the use of BB+5% FBS resulted in significantly more biofilm biomass. Also, no significant differences were found between day 3 and day 5 for the use of BB+5%FBS (**Figure 3.4**).

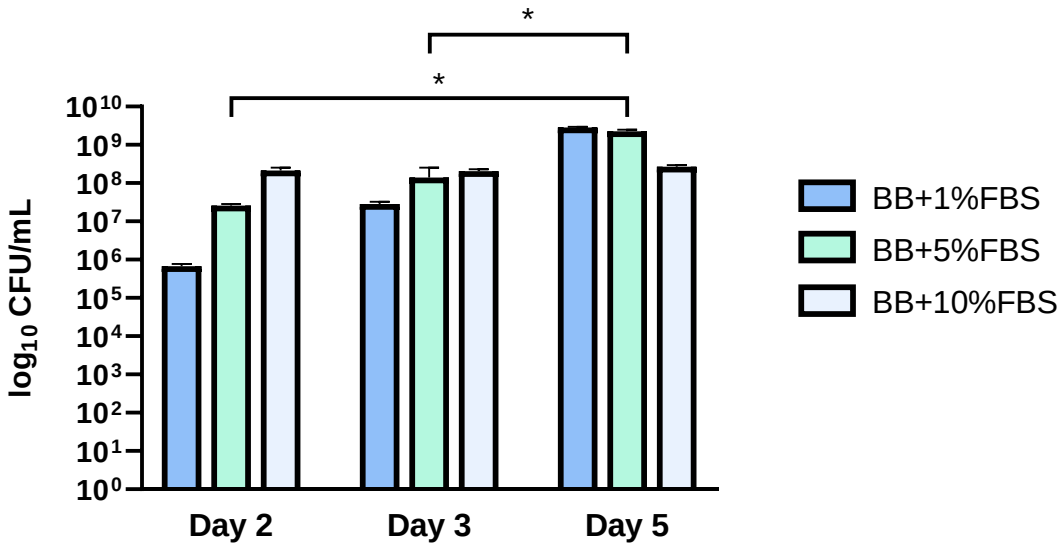

Figure 3.5 – Viable bacteria quantification in the biofilm. Viable bacteria in the biofilm were determined by CFU counting, at 2, 3 and 5 days of biofilm growth and in liquid medium (Brucella broth, BB) supplemented with different concentrations of FBS (1%, 5% and 10% v/v). There are statistically significant differences between all time-points for biofilms grown in BB+1%FBS. *p<0.05, statistically significant differences between the number of viable bacteria between conditions.

Biofilms grown in BB+1%FBS show a significant increase in the number of viable bacteria throughout the 3 time-points, while biofilms grown in BB+10% FBS show no significant changes. For BB+5% FBS, the number of viable bacteria is the highest at the day 5 time-point and significantly different from day 2 and day 3 time-points.

Nevertheless, due to the significant number of viable bacteria and biofilm biomass already present on day 3, the fact that the biofilm has already reached a mature status and taking into account the fastidious growth of *H. pylori*, this time-point was selected to expedite the biofilm growth process for subsequent assays. The selected media was BB+5% FBS since it induced the most biomass formation.

3.3. Effects of NLC on *H. pylori* biofilms

After the selection of the optimal conditions for the preparation of the biofilm, *H. pylori* biofilms were exposed to NLC (U-NLC and DHA-NLC). The effect of NLC treatment was evaluated by total biomass quantification using the CV assay (**Figure 3.6**) and the number of viable cells by CFU counting and calculation of CFUs/mL (**Figure 3.7**).

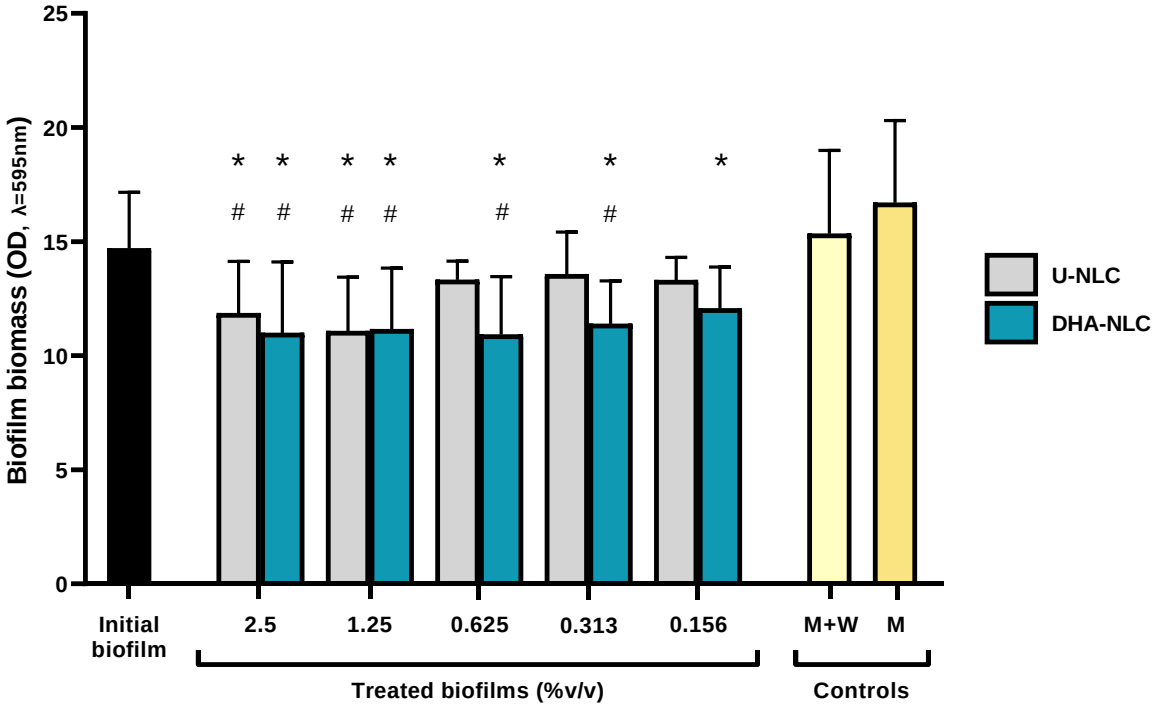

Figure 3.6 - Effect of NLC on the total biofilm biomass quantified by the CV assay (OD, λ= 595 nm). Nanoparticle concentrations are expressed in % v/v. M – media control (BB+5%FBS), M+W – BB+5%FBS control with water in equivalent volume to NLC suspension for the concentration of 40 %v/v. * p<0.05, significantly different from the media control. # p<0.05, significantly different from the initial biofilm. No significant differences were found between the M and the M+W controls. n=3

Previous to the quantification of the biofilm biomass, the ability of CV to stain the nanoparticles was evaluated and no influence was observed (data not shown).

The results indicate that the NLC have a significant inhibitory effect on biofilm biomass shown by the differences between the treated biofilms and the controls. U-NLC had an inhibitory effect in concentrations starting at 1.25% v/v ($7.35x10^{12}$ particles/mL), while DHA-NLC had an inhibitory effect in all of the concentrations tested.

Simultaneously, the treatment with NLC causes a significant reduction of the biofilm biomass in most of the concentrations tested, shown by the differences between the treated biofilms and the initial biofilm. Biofilms treated with U-NLC had up to 25% less biomass and this reduction started at a concentration of 1.25% v/v ($7.35x10^{12}$ particles/mL). Meanwhile, for biofilms treated with DHA-NLC, these had up to 26% less biomass and reduction started at a concentration of 0.313% v/v ($1.12x10^{12}$ particles/mL).

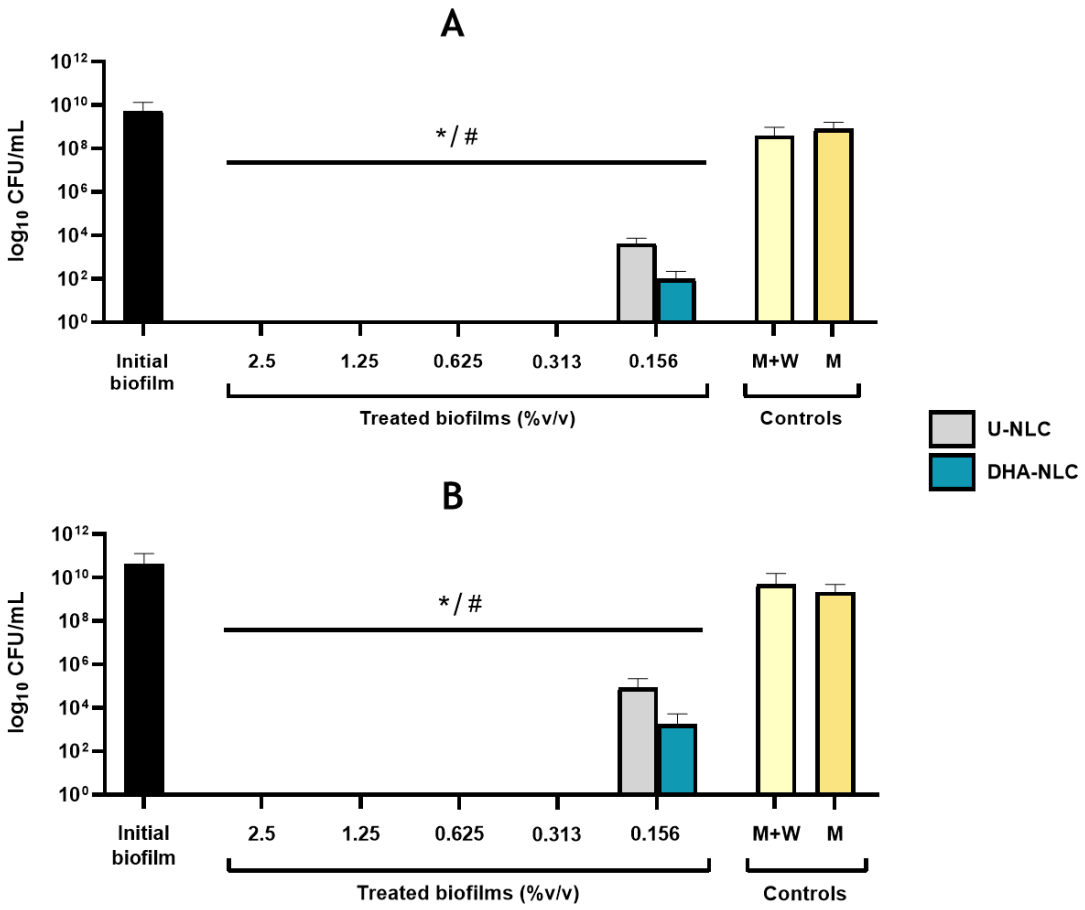

Figure 3.7 - Effect of NLC on (A) planktonic and (B) biofilm viable bacteria, measured by CFUs. Nanoparticle concentrations are expressed in % v/v. M – media control (BB+5%FBS), M+W – BB+5%FBS control with water in equivalent volume to NLC suspension for the concentration of 40% v/v. * $p<0.05$, significantly different from the media control. # $p<0.05$, significantly different from the initial biofilm. No significant differences were found between the M and the M+W controls. n=3

For planktonic bacteria (**Figure 3.7A**), the minimal inhibitory concentration (MIC) is defined as the lowest concentration at which visible bacterial growth does not occur. The minimal bactericidal concentration (MBC) is defined as the lowest concentration at which bacterial growth does not occur and additionally the initial viability is reduced by at least 99.9% (≥ 3 $\log_{10}$) (136). NLC were bactericidal in all the concentrations tested, with the MBC being established at a concentration of 0.156 %v/v ($7.35x10^{12}$ and $4.49x10^{12}$ particles/mL, for U-NLC and DHA-NLC respectively). This does not differ much from previous results with planktonic *H. pylori* J99 strain, which had a MBC of 0.5 %v/v (the lowest concentration tested) (137).

In terms of biofilm (**Figure 3.7B**), the minimal biofilm inhibitory concentration (MBIC) is defined as the lowest concentration at which there is no time-dependent increase in the number of biofilm viable bacteria. On the other hand, the biofilm bactericidal concentration (BBC) is the lowest concentration that kills 99.9% of the cells recovered from a biofilm culture compared to the growth control, while the minimal biofilm eradication concentration is the lowest concentration required to completely eradicate the biofilm (138). The obtained results reveal that despite there is biofilm biomass in all of the treated biofilms, the bacteria embedded in it are not viable. Therefore, the BBC was established at a concentration of 0.156% v/v ($7.35x10^{12}$ and $4.49x10^{12}$ particles/mL, for U-NLC and DHA-NLC respectively). Treatment of the biofilms with free DHA was also tested and the MBC and BBC were established at 12.5 and 25 μM, the equivalent amount found in DHA-NLC at 0.625% and 1.25% v/v, respectively (data not shown).

Biofilms were further analyzed using SEM (**Figure 3.8**).

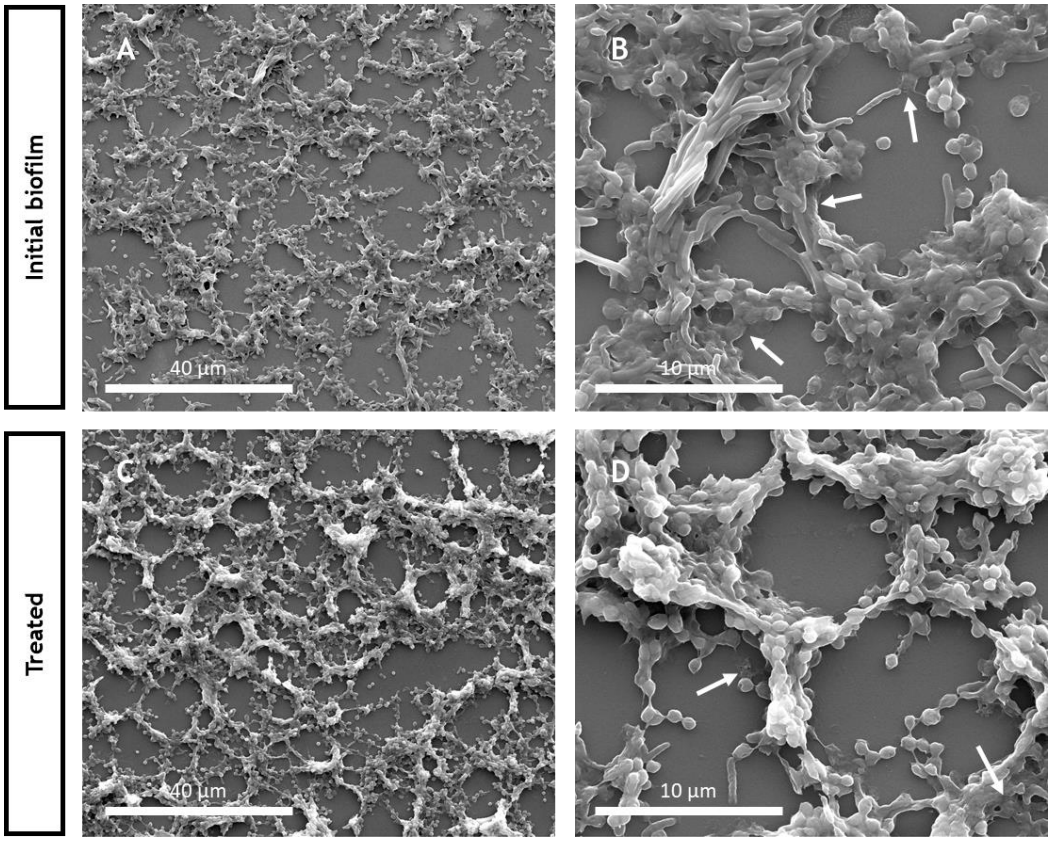

Figure 3.8 - SEM images of initial (A,B) and treated with 0.156% v/v U-NLC (C,D) *H. pylori* J99 biofilms. A,C: 2500x magnification and scale bar represents 40 µm. B,D: 10000x magnification and scale bar represents 10 µm. Arrows are pointing to the EPS.

Through SEM imaging, the biofilm structure could be seen in detail, including the visualization of some EPS covering and connecting bacteria (**Figure 3.8**).

Although both biofilms, initial and treated, have bacteria in coccoid shape, it seems that most of the bacillar bacteria in the initial biofilm convert into a coccoid shape when exposed to NLC (**Figure 3.8 B and D**).

Biofilms were further analyzed using CLSM. A representative image of a LIVE/DEAD stain is shown in **Figures 3.9** and **3.10.**

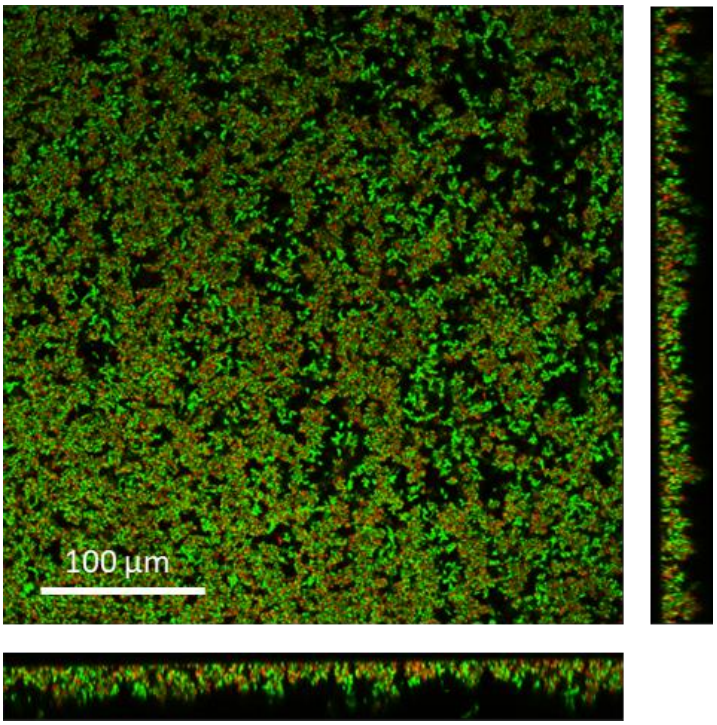

Figure 3.9 – CLSM image of *H. pylori* J99 biofilm with orthogonal views. Biofilm was fixed with PFA at 4% v/v and stained with a LIVE/DEAD kit (SYTO 9/PI). Alive bacteria are shown in green and dead bacteria are shown in red. Scale bar: 100 µm.

This image highlights some biofilm characteristics, such as its irregular structure with mushroom-like structures (**Figure 3.9**), which allows for the circulation of gases and nutrients into the deeper layers of the biofilm. Nevertheless, a significant number of dead bacteria are expected, since this circulation is limited and unable to reach all bacteria.

In **Figure 3.10**, when the biofilm control is compared with the treated biofilms, an increase in the number of dead bacteria is noticeable after exposure to NLC. However, the reduction in bacterial viability in treated biofilms is not as high as the one obtained in the negative control, where bacterial death was induced by nutrient starvation (treatment with PBS) to obtain a high number of dead bacteria and used to adjust the fluorescence intensity of PI.

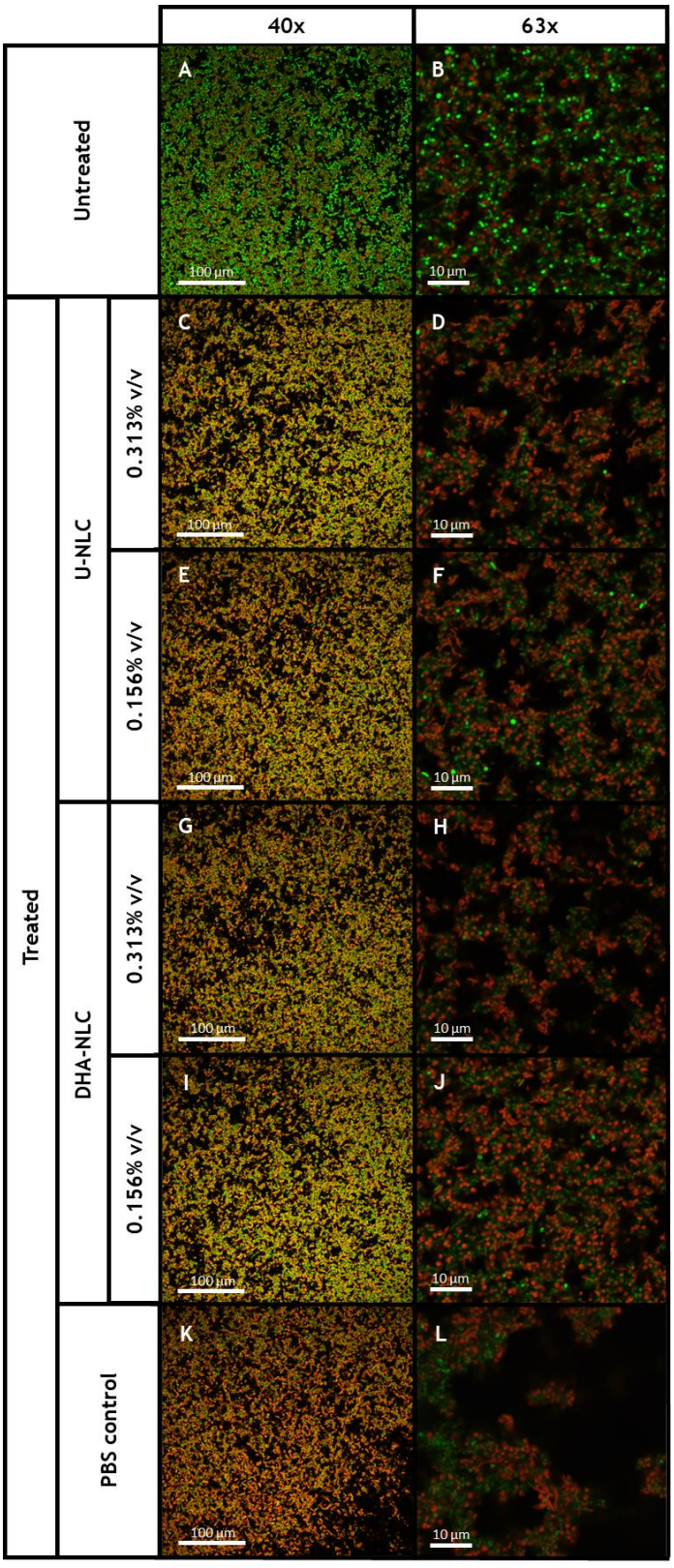

Figure 3.10 – CLSM images of *H. pylori* J99 biofilms untreated and treated with NLC. Biofilms were fixed with PFA at 4% v/v and stained with a LIVE/DEAD kit (SYTO 9/PI). Alive bacteria are shown in green and dead bacteria are shown in red. A, C, E, G, I, K: 40x ocular and scale bar 100 µm. B, D, F, H, J, L: 63x ocular and scale bar 10 µm.

Interestingly, these images do not translate into the above-mentioned CFU results (**Figure 3.7B**), since there are still live bacteria (green) in the biofilm as seen by CLSM, while no viable bacteria

were detected by CFU counting. This discrepancy may be a result of the *H. pylori's* ability to convert into a viable but non-culturable (VBNC) state.

Chapter 4 - Discussion

H. pylori is one of the strongest known risk factors for the development of gastric cancer (7). As such, it is thought that eradicating *H. pylori* infection could lead to a dramatic reduction in the incidence of gastric cancer and other *H. pylori*-associated gastrointestinal disorders (139, 140).

The recently discovered ability of *H. pylori* to form biofilms brings up new challenges in infection treatment (76). In general, biofilm-associated bacteria show increased resistance to antimicrobials that can be linked to several factors. For instance, the matrix prevents an easy and fast diffusion of these compounds. Also, bacteria in biofilms can suffer changes in metabolism, reducing the uptake of these substances and, the proximity of bacteria and the environment provided by the biofilm allows for enhanced horizontal gene transfer, which might increase bacterial virulence (132). When coupled with the increasing resistance of bacteria to antibiotics (50, 141), this leads to a further decrease in eradication rates and a pressing need for alternative treatments that are able to eradicate planktonic bacteria as well as bacteria embedded in a biofilm.

H. pylori biofilms have a decrease in susceptibility to the most commonly used antibiotics when compared with planktonic bacteria. The minimal bactericidal concentrations were found to suffer an increase of up to 4, 8 and 2-fold for clarithromycin, amoxicillin and metronidazole, respectively (69, 142). Recently, there has been an increase in the research of natural compounds to be used as alternatives for conventional antibiotic treatment of *H. pylori* infection. Fatty acids are an example of natural compounds that have a bactericidal effect and a broad spectrum of activity (143). The subcategory of polyunsaturated fatty acids (PUFA) includes some compounds, such as docosahexaenoic acid (DHA), an omega-3 PUFA present in fish oil. DHA has demonstrated to be able to inhibit *H. pylori* growth *in vitro* and *in vivo* in a dose-dependent manner (129). However, its efficacy may be compromised by the loss of bioactivity since its highly unsaturated structure makes them easy targets for oxidation. Therefore, when administered by the oral route, these substances suffer alterations from exposure to environmental factors such as oxygen, light and pH changes (gastric acid) (144).

A nanotechnological approach to these lipophilic bioactive compounds can help with their stability and, as a consequence, improve drug bioavailability. Nanostructured lipid carriers (NLC) were developed to encapsulate DHA and this strategy demonstrated to have a bactericidal effect at low concentrations on planktonic bacteria, hinting at the great potential in the treatment of *H. pylori* infection (130). Moreover, U-NLC also had a bactericidal effect on *H. pylori* although their action was slower than DHA-NLC (130, 131).

In this work, it was explored if the bactericidal effect of the NLC could be extended to *H. pylori* embedded in a biofilm, with all of the challenges that this extra mechanism of defense poses.

NLC were produced by hot homogenization and ultrasonication without the use of organic solvents. NLC are composed of lipids recognized as safe by the FDA and they are biocompatible and

biodegradable, advantages that contribute to their safety. Also, in the case of DHA-NLC, they are able to protect the DHA molecules from degradation by the harsh environment of the stomach, being an excellent delivery system for the oral route (109). Nanoparticles' ability to overcome biological barriers, such as the mucus layer in the stomach, due to their size in the nano-scale is yet another advantage in the targeting of *H. pylori* (145). When it comes to the penetration of the biofilm matrix, the ability of the NLC to reach bacteria in the deeper layers of the biofilm might influence their bactericidal effects. There is a complex interplay of factors that influence the transport of nanoparticles in the biofilm matrix, among them the size and charge of the nanoparticles and the viscosity, porosity and cell density of the EPS matrix (146).

Characterization of the NLC showed monodisperse suspensions of nanoparticles, PdI inferior to 0.3 (117), with diameters of 255±16 nm and 346±23 nm for U-NLC and DHA-NLC respectively. Nanoparticles with diameters up to 130 nm have shown to have great penetration ability, nonetheless, nanoparticles which do not exceed 500 nm in diameter can still effectively penetrate the biofilm matrix (147). The NLC developed are in this size range and they seem to have penetrated the biofilm to some extent during the 24h of exposure, causing the inhibition and reduction of the total biomass, as well as a significant reduction in the number of viable cells.

In terms of surface charge, the average zeta potential (ZP) was -32±2 mV and -21±1 mV for U-NLC and DHA-NLC, respectively. A ZP of -30 mV is considered as optimum for a stable nanoparticle suspension. Nevertheless, lipid nanoparticle suspensions with ZP between -20 and -40 mV are still considered stable and less likely to form aggregates or change size (148). As such, the obtained NLC suspensions were stable and showed no aggregation, as was possible to observe in the videos obtained for NTA while determining nanoparticle concentration. The addition of DHA causes changes in the surface charge of the NLC, slightly increasing the ZP. Since the biofilm matrix is negatively charged as a whole because of eDNA and some polysaccharides and despite the advantages of having a ZP of around -30 mV for suspension stability, it can lead to electrostatic repulsion between the NLC and the matrix and result in an unwanted outcome, a slower diffusion of the nanoparticles (146, 149, 150).

Since no previous study involving these NLC and *H. pylori* biofilms was reported, this work started with the establishment of a low complexity mature biofilm model, in a closed environment without any added substrate (e. g. metal coupons) and without a continuous flow of fresh media (151). For that, biofilms were grown in polystyrene plates, a substrate is shown to induce good biofilm formation (62). Due to the lack of a standardized protocol for susceptibility testing in biofilms, the production of a biofilm model for this work required optimization, namely in the growth conditions to obtain a mature biofilm.

H. pylori is a bacterium of fastidious growth, requiring a complex nutrient-rich medium and microaerophilic conditions (<5% O_2) for its culture (152). Brucella broth (BB) is commonly used as a liquid medium for *H. pylori* growth, however, despite its abundance of nutrients, it is commonly supplemented with fetal bovine serum (FBS). This supplement adds an important component to the mixture of nutrients that support bacterial growth, cholesterol. It is known that *H. pylori* takes up cholesterol and incorporates it into its membrane. Also, it has been shown that the presence of cholesterol in the media leads to an optimum growth of *H. pylori* (153). Nutrient starvation is an environmental stressor that can induce *H. pylori* to form biofilms (135). As such, reducing the amount of serum added to the medium as supplementation for optimal bacterial growth can be a way of mimicking this stress and has been correlated with an increase in biofilm production (62, 135). Our results show that a decrease in FBS supplementation, using 5% v/v FBS, increased the amount of biofilm biomass. For supplementation with 1% and 10% v/v FBS biofilm biomass was significantly lower. Although for 1% v/v FBS the number of viable bacteria in the biofilm increases in a time-dependent way, biofilm matrix production might be impaired by the lack of cholesterol

(153). On the other hand, for 10% v/v FBS the number of viable bacteria in the biofilm remains high and constant throughout all time-points, as it is the optimal supplementation for *H. pylori* viability and growth, but matrix production remains similar to 1% v/v FBS and is not as high as for 5% v/v FBS.

Biofilm formation is also dependent on time, as biofilms go through different stages, from early to intermediate and, finally, to mature biofilms. At the early stage, the bacteria start aggregating and adhering to each other, forming microcolonies. In the intermediate stage, bacteria start multiplying and producing the extracellular matrix. A mature biofilm is a biofilm composed of a stable number of bacteria encased with matrix (up to 90% of the total biofilm volume), which can suffer disruption leading to the release of bacteria from its structure (154). The comparison between 2 days and 3/5 days of *H. pylori* biofilm growth in terms of viable bacteria show differences, however, these are not as steep as the differences observed between total biofilm biomass. This can mean that the *H. pylori* J99 biofilm with 2 days of growth is mainly composed of bacteria adhered to each other and only when transitioning to 3 days of growth does it start to produce and secrete EPS in large quantities. As such, after 2 days of growth, this biofilm can be classified as intermediate. Since increased biofilm biomass and the release of bacteria from the biofilm are considered characteristics of a mature biofilm, we considered that from day 3 onwards, the *H. pylori* biofilm was mature. SEM analysis confirms the presence of EPS in the biofilm, connecting the bacteria, after 3 days of growth.

Although the MIC and MBC have been previously determined for the *H. pylori* J99 and other *H. pylori* strains (130) (**Appendices I and II**), it was expected that killing the bacteria in the biofilm would require a higher concentration of NLC due to the above-mentioned characteristics that improve biofilm resistance to treatment.

Analysis of the biofilm biomass after treatment showed that NLC have a significant inhibitory effect on biofilm biomass and were able to reduce it. Inhibition is seen by the lack of growth above the initial biofilm's biomass when compared with the possible growth, i.e. the media control that represents the expected growth had the biofilm not been treated. While U-NLC inhibited the biofilm growth at concentrations of 1.25% v/v and higher, DHA-NLC caused inhibition on the full range of concentrations tested, being 0.156% v/v the lowest one. A more clinically relevant measurement of NLC efficacy is its ability to reduce the biomass of the initial biofilm, since the goal of the treatment is the eradication of the biofilm and not only its inhibition. Biofilms after treatment had up to 25% or 26% less biomass than the initial biofilm, for U-NLC and DHA-NLC, respectively. While for U-NLC reduction occurred for concentrations starting at 1.25% v/v, for DHA-NLC it occurred for concentrations starting at 0.313% v/v and higher. Bacteria that remain in the biofilm, whether dead or alive, are quantified as biofilm biomass by this assay together with the extracellular matrix. As such, it is expected that any reduction of biomass results from the degradation of the matrix and the resulting release of bacteria, although the determination of this NLC effect would require further research to determine the exact mechanism of action on the EPS and its components.

Also, bacteria can suffer metabolic and genetic changes in the microenvironment of the biofilms, possibly resulting in different susceptibility to antimicrobial agents. Since the mature biofilms release bacteria subjected to these processes, it was important to evaluate any possible changes in the bactericidal effect of NLC. For that, the MBC of the NLC against the planktonic bacteria released by the biofilm was evaluated and established at a concentration of 0.156 %v/v. Previous results with planktonic *H. pylori* J99 strain demonstrated an MBC of 0.5 %v/v, which was the lowest concentration tested (130). Therefore, the MBC of 0.156%v/v here obtained corroborates that NLC remain effective against bacteria released from the biofilms.

Regarding the biofilms, treatment with NLC at all the concentration tested had a bactericidal effect, establishing the BBC at a concentration of 0.156 %v/v for NLC. Treatment of the biofilms

with free DHA was also tested and the BBC was established at a concentration of 0.625 %v/v, significantly higher than the BBC established for both NLC. This shows that in addition to protecting this compound from degradation, the NLC enhances its bacterial effect, and in the case of biofilms it might enhance its effect.

When comparing the performance of U-NLC and DHA-NLC, the presence of DHA leads to the significant inhibition of the *H. pylori* biofilm biomass at all the concentrations tested (2.5 to 0.156% v/v) and a significant reduction of biomass starting at 0.313% v/v, both lower concentrations than for U-NLC. This difference might be a result of the synergy between the NLC itself and the DHA. Once the DHA is released from the NLC, its smaller dimensions compared to the nanoparticles might increase its diffusion through the matrix. Also, fatty acids have been shown to reduce the biofilm of several pathogens through changes in the expression of genes involved in biofilm formation (155).

In addition to CFU determination, the analysis of the biofilms using CLSM and LIVE/DEAD staining gives qualitative information about the viability, morphology and organization of the bacteria in the biofilm. The images obtained for the treated biofilms show more live bacteria (in green) than detected by the CFU counting. Also, observing SEM images, there seems to be an increase in coccoid morphology in the biofilms treated with NLC compared to the untreated ones. CFU counting only accounts for viable culturable bacteria and not necessarily all of the live bacteria. Since CLSM still detected live bacteria and there seems to be a shift in morphology from bacillar to coccoid, this leads to the assumption that some of these bacteria have entered a viable but non-culturable (VBNC) state. The transition into this state might lead to an underestimation of the number of viable bacteria and in turn lead to a lower BBC that is not accurate. This would explain why the BBC is so similar to the previously determined MBC for planktonic bacteria despite the obstacles posed by the biofilm.

The exact mechanism of action of the NLC is still unknown, but it has been reported that they cross the bacterial membranes and destabilize them, leading to cytoplasmic leakage and cell death (131). When *H. pylori* converts into a VBNC state it suffers changes in its bacterial wall, preventing the action of substances such as antibiotics (30) and possibly preventing the changes caused by the NLC. Previous results by Seabra *et al*. show bacterial death of *H. pylori* in a bacillar conformation and suggest that the fast effect of the DHA-NLC prevented the modification of the bacterial cell wall into a coccoid conformation (130). In the case of biofilms, and as previously mentioned, the size and negative charge of the NLC might be constraints in its action and can slow down diffusion. It is thought that the NLC effect has a similar time frame of action on the upper layers of the biofilm as with planktonic bacteria, but it takes much longer for the NLC to reach the bacteria in the deeper layers of the biofilm. As such, these bacteria have more time to suffer morphological changes into a form of *H. pylori* more resistant to treatment. To increase the effectiveness of the NLC and surpass the barrier of the EPS matrix, treatment with NLC could be conjugated with a substance such as N-acetylcysteine which has a demonstrated effect of disrupting the matrix of biofilms (156).

Moreover, the three-dimensional structure of the biofilm was examined using SEM and CLSM showing the irregular structure composed of mushroom-like colonies surrounded by channels typical of most biofilms. These channels allow for the diffusion of nutrients and gases in the different layers that compose the biofilms. Nevertheless, biofilms contain both live and dead bacteria, with this ratio varying depending on their position in the biofilm. Images seem to show a predominance of the coccoid shape in the deeper layers of the biofilm, where it is harder for nutrients to diffuse despite the formation of channels (79). Additionally, the LIVE/DEAD staining used also offers some limitations such as the adverse effects on the viability of bacteria when left in the presence of propidium iodide (PI) overtime, and the ability of PI to also stain extracellular DNA, one of the components of the biofilm matrix (157, 158). This can lead to an overestimation of the number of

dead bacteria in the biofilm. Nevertheless, previous to treatment and as detected by SEM, it seems that the deeper layers of the biofilm have a higher ratio of coccoid shaped bacteria than bacillar bacteria. These bacteria might be dead, as was previously mentioned, but they might also be in a VBNC state due to stress conditions, such as lack of nutrients or anaerobic conditions (30). Research on this VBNC state has shown that it is not always permanent and *H. pylori* retains its virulence and ability to return to an infective state (29). The survival of these coccoid bacteria after treatment could lead to the reformation of the biofilm. This is something that needs to be further evaluated in the future.

This work was able to demonstrate the ability of the NLC to kill both planktonic and biofilm bacteria at low concentrations, proving that the NLC are able to penetrate the biofilm matrix and reach bacteria in the most interior layers of the biofilm. Although the main purpose of the developed NLC was an application in the treatment of gastric infection caused by *H. pylori*, these results in the context of biofilms and the current knowledge about the different environments where *H. pylori* biofilms may be present can lead to extrapolation into different and broader applications of this strategy. For example, NLC could be used to treat oral biofilms or biofilms formed in water supply systems by *H. pylori*, which could reduce the risk that these create of reinfection or dissemination of infection. The overall result would be a more effective eradication of *H. pylori* both in the human body and outside of it without resourcing to the use of antibiotics and the burden of their associated drawbacks.

Chapter 5 – Conclusions and future work

Conclusions

Current therapies for the treatment of *H. pylori* infection show increasing failure rates due to the bacteria's acquisition of resistance to conventional antibiotics. Also, recent studies highlighted the role that biofilms can play in infection resistance to treatment and reinfection. New strategies are required to overcome these problems. They should be able to withstand the gastric pH range and gastric emptying, avoid the formation of resistance mechanisms and be able to reach *H. pylori* protected by either the gastric mucosa or a biofilm. A possible strategy is the use of NLC.

Unloaded NLC (U-NLC) and NLC loaded with docosahexaenoic acid (DHA-NLC) were produced and characterized. Characterization showed monodisperse suspensions of nanoparticles with diameters of approximately 255 ± 16 nm and 346 ± 23 nm and a surface charge of approximately -32 ± 2 mV and -21 ± 1 mV, for U-NLC and DHA-NLC, respectively.

This work aimed to evaluate the effect of NLC on mature *H. pylori* biofilms. To do so, a mature biofilm model was successfully created and characterized in terms of total biofilm biomass and the number of viable bacteria. The growth conditions were optimized, resulting in the selection of 3 days for the growth of the model biofilms and Brucella broth supplemented with 5% fetal bovine serum.

Using this model, results show that NLC were able to inhibit and reduce the biomass of *H. pylori* J99 biofilms as well as kill all surrounding planktonic bacteria and reduce the number of viable bacteria embedded in the biofilms. For both planktonic bacteria and bacteria embedded in the biofilm, the minimal bactericidal concentration (MBC) and the biofilm bactericidal concentration (BBC), respectively, were established at a concentration of 0.156% v/v.

Further analysis, using microscopy techniques such as SEM and CLSM, has led to the hypothesis that *H. pylori* is able to convert into a VBNC state and avoid some of the NLC effects. This can have consequences in biofilm eradication since bacteria might be able to revert to an active state and regrow the biofilm, restarting the infection, and should be further explored.

The potential of U-NLC and DHA-NLC was further demonstrated, namely in the context of biofilms, highlighting that they should be pursued within the scope of management of *H. pylori* infection.

Future work

Further confirmation and investigation of the conversion of *H. pylori* bacteria into a viable but non-culturable state, when exposed to NLC would bring more insight into biofilm behavior as a resistance mechanism. Evaluation of the biofilm's ability to regrow after stopping the treatment would be important to determine if the NLC inhibitory is permanent or only temporary. On the other hand, longer exposure times to treatment with NLC could be evaluated to determine if biofilm eradication is time dependent.

A deeper characterization of the biofilm's EPS composition, before and after treatment, could help in drawing further conclusions about the biomass reduction induced by the NLC. The ability of the NLC to penetrate the biofilm matrix should also be evaluated.

Taking into account that *H. pylori* infection is typically multistrain (159, 160) and most of the studied strains are able to form biofilms, it would be of interest to evaluate biofilm formation in co-cultures with different *H. pylori* strains and the effect that NLC would have on these biofilms.

Besides multistrain biofilms, increasing the complexity of the biofilm model by adding mucins (106, 132) would allow for a more realistic evaluation of both the formation of the *H. pylori* biofilm and the ability of NLC to reach the bacteria through the mucus and the EPS.

Also, since it is known that environmental *H. pylori* biofilms, such as the ones found in water delivery systems, can be responsible for transmitting infection, NLC could be tested as a biofilm treatment strategy in these conditions.

Finally, NLC specificity towards *H. pylori* was evaluated by testing their effectiveness against a variety of bacteria from the gut microbiome. However, *H. pylori* has plenty of characteristics that make it an unique pathogen and very different from other bacteria. To further evaluate this potential treatment's specificity it would be interesting to test its effect on a bacterium that shares more characteristics with *H. pylori* and is taxonomically closer to it, such as *Campylobacter jejuni*.

References

1. Kusters JG, van Vliet AH, Kuipers EJ. Pathogenesis of Helicobacter pylori infection. Clinical microbiology reviews. 2006;19(3):449-90.
2. Horemans T. A quest for novel therapeutic and diagnostic approaches in Helicobacter pylori infections. 2014.
3. Warren JR, Marshall BJTl. Unidentified curved bacilli on gastric epithelium in active chronic gastritis. 1983;321(8336):1273-5.
4. Goodwin CS, Armstrong JA, Chilvers T, Peters M, Collins MD, Sly L, et al. Transfer of Campylobacter pylori and Campylobacter mustelae to Helicobacter gen. nov. as Helicobacter pylori comb. nov. and Helicobacter mustelae comb. nov., respectively. International Journal of Systematic Evolutionary Microbiology. 1989;39(4):397-405.
5. Møller H, Heseltine E, Vainio H. Working group report on schistosomes, liver flukes and Helicobacter pylori. Meeting held at IARC, LYON, 7–14 june 1994. International Journal of Cancer. 1995;60(5):587-9.
6. International Agency for Research on Cancer. Globocan Worldwide Fact Sheet 2018. In: Organization WH, editor. 2018.
7. Balakrishnan M, George R, Sharma A, Graham DYJCgr. Changing trends in stomach cancer throughout the world. 2017;19(8):36.
8. Eslami M, Yousefi B, Kokhaei P, Arabkari V, Ghasemian A. Current information on the association of Helicobacter pylori with autophagy and gastric cancer. Journal of cellular physiology. 2019.
9. Molnar B, Galamb O, Sipos F, Leiszter K, Tulassay Z. Molecular Pathogenesis of Helicobacter pylori Infection: The Role of Bacterial Virulence Factors. Digestive Diseases. 2010;28(4-5):604-8.
10. Correa P, Piazuelo MB. The gastric precancerous cascade. Journal of digestive diseases. 2012;13(1):2-9.
11. O'Connor A, O'Morain CA, Ford AC. Population screening and treatment of Helicobacter pylori infection. Nature Reviews Gastroenterology &Amp; Hepatology. 2017;14:230.
12. Vaziri F, Tarashi S, Fateh A, Siadat SD. New insights of Helicobacter pylori host-pathogen interactions: The triangle of virulence factors, epigenetic modifications and non-coding RNAs. World J Clin Cases. 2018;6(5):64-73.
13. Amieva M, Peek RM, Jr. Pathobiology of Helicobacter pylori-Induced Gastric Cancer. Gastroenterology. 2016;150(1):64-78.
14. Vogiatzi P, Cassone M, Luzzi I, Lucchetti C, Otvos L, Jr., Giordano A. Helicobacter pylori as a class I carcinogen: physiopathology and management strategies. Journal of cellular biochemistry. 2007;102(2):264-73.
15. Hooi JKY, Lai WY, Ng WK, Suen MMY, Underwood FE, Tanyingoh D, et al. Global Prevalence of Helicobacter pylori Infection: Systematic Review and Meta-Analysis. Gastroenterology. 2017;153(2):420-9.
16. Zamani M, Ebrahimtabar F, Zamani V, Miller WH, Alizadeh-Navaei R, Shokri-Shirvani J, et al. Systematic review with meta-analysis: the worldwide prevalence of Helicobacter pylori infection. Alimentary pharmacology & therapeutics. 2018;47(7):868-76.
17. Kotilea K, Bontems P, Touati E. Epidemiology, Diagnosis and Risk Factors of Helicobacter pylori Infection. 2019.
18. Morais S, Ferro A, Bastos A, Castro C, Lunet N, Peleteiro B. Trends in gastric cancer mortality and in the prevalence of Helicobacter pylori infection in Portugal. Eur J Cancer Prev. 2016;25(4):275-81.

19. Bastos J, Peleteiro B, Barros R, Alves L, Severo M, de Fátima Pina M, et al. Sociodemographic Determinants of Prevalence and Incidence of Helicobacter pylori Infection in Portuguese Adults. Helicobacter. 2013;18(6):413-22.
20. Vale FF, Vitor JM. Transmission pathway of Helicobacter pylori: does food play a role in rural and urban areas? International journal of food microbiology. 2010;138(1-2):1-12.
21. Goh KL, Chan WK, Shiota S, Yamaoka Y. Epidemiology of Helicobacter pylori infection and public health implications. Helicobacter. 2011;16 Suppl 1(0 1):1-9.
22. Mladenova-Hristova I, Grekova O, Patel A. Zoonotic potential of Helicobacter spp. Journal of microbiology, immunology, and infection = Wei mian yu gan ran za zhi. 2017;50(3):265-9.
23. Talaei R, Souod N, Momtaz H, Dabiri H. Milk of livestock as a possible transmission route of Helicobacter pylori infection. Gastroenterology and hepatology from bed to bench. 2015;8(Suppl 1):S30-6.
24. Schreiber S, Bucker R, Groll C, Azevedo-Vethacke M, Garten D, Scheid P, et al. Rapid loss of motility of Helicobacter pylori in the gastric lumen in vivo. Infection and immunity. 2005;73(3):1584-9.
25. Syafiq F, Morris N, Murphy A, Kennedy J. Development of Amoxicillin loaded microspheres for anti-Helicobacter pylori infection using Ionic Gelation method2017. 56-67 p.
26. O'Rourke J, Bode G. Morphology and Ultrastructure. In: Mobley HLT, Mendz GL, Hazell SL, editors. Helicobacter pylori: Physiology and Genetics. Washington (DC): ASM Press; 2001.
27. O'Toole PW, Clyne M. Cell Envelope. In: Mobley HLT, Mendz GL, Hazell SL, editors. Helicobacter pylori: Physiology and Genetics. Washington (DC): ASM Press; 2001.
28. Chmiela M, Walczak N, Rudnicka K. Helicobacter pylori outer membrane vesicles involvement in the infection development and Helicobacter pylori-related diseases. Journal of biomedical science. 2018;25(1):78.
29. Cellini L. Helicobacter pylori: a chameleon-like approach to life. World J Gastroenterol. 2014;20(19):5575-82.
30. Hirukawa S, Sagara H, Kaneto S, Kondo T, Kiga K, Sanada T, et al. Characterization of morphological conversion of Helicobacter pylori under anaerobic conditions. Microbiology and Immunology. 2018;62(4):221-8.
31. Testerman TL. Chapter 8 - Helicobacter pylori. In: Gavins FNE, Stokes KY, editors. Vascular Responses to Pathogens. Boston: Academic Press; 2016. p. 87-109.
32. Andersen LP, Wadstrom T. Basic Bacteriology and Culture. In: Mobley HLT, Mendz GL, Hazell SL, editors. Helicobacter pylori: Physiology and Genetics. Washington (DC): ASM Press, Washington (DC); 2001.
33. Huang Y, Wang Q-l, Cheng D-d, Xu W-t, Lu N-h. Adhesion and Invasion of Gastric Mucosa Epithelial Cells by Helicobacter pylori. Frontiers in cellular and infection microbiology. 2016;6(159).
34. Yamaoka Y. Roles of Helicobacter pylori BabA in gastroduodenal pathogenesis. World journal of gastroenterology. 2008;14(27):4265-72.
35. Chang WL, Yeh YC, Sheu BS. The impacts of H. pylori virulence factors on the development of gastroduodenal diseases. J Biomed Sci. 2018;25(1):68.
36. Thamphiwatana, Gao W, Pornpattananangkul D, Zhang Q, Fu V, Li J, et al. Phospholipase A2-responsive antibiotic delivery via nanoparticle-stabilized liposomes for the treatment of bacterial infection. J Mater Chem B. 2014;2(46):8201-7.
37. Khan S, Karim A, Iqbal S. Helicobacter urease: Niche construction at the single molecule level2009. 503-11 p.
38. Zarzecka U, Modrak-Wójcik A, Figaj D, Apanowicz M, Lesner A, Bzowska A, et al. Properties of the HtrA Protease From Bacterium Helicobacter pylori Whose Activity Is Indispensable for Growth Under Stress Conditions. Front Microbiol. 2019;10:961.
39. Lina TT, Alzahrani S, Gonzalez J, Pinchuk IV, Beswick EJ, Reyes VE. Immune evasion strategies used by Helicobacter pylori. World J Gastroenterol. 2014;20(36):12753-66.
40. Appelmelk B, Vandenbroucke-Grauls C. H pylori and Lewis antigens. Gut. 2000;47(1):10-1.
41. Hatakeyama M. Structure and function of Helicobacter pylori CagA, the first-identified bacterial protein involved in human cancer. Proc Jpn Acad Ser B Phys Biol Sci. 2017;93(4):196-219.
42. Seyler RW, Jr., Olson JW, Maier RJ. Superoxide dismutase-deficient mutants of Helicobacter pylori are hypersensitive to oxidative stress and defective in host colonization. Infect Immun. 2001;69(6):4034-40.
43. Talebi Bezmin Abadi A. Therapy of Helicobacter pylori: present medley and future prospective. BioMed research international. 2014;2014:124607.
44. Sugiyama T. Proton pump inhibitors: Key ingredients in Helicobacter pylori eradication treatment. Proton Pump Inhibitors: A Balanced View. 32: Karger Publishers; 2013. p. 59-67.

45. Verma A, Dubey J, Hegde RR, Rastogi V, Pandit JK. Helicobacter pylori: past, current and future treatment strategies with gastroretentive drug delivery systems. Journal of drug targeting. 2016;24(10):897-915.
46. Smith SM, O'Morain C, McNamara D. Helicobacter pylori resistance to current therapies. Current opinion in gastroenterology. 2019;35(1):6-13.
47. Group EHpS. Current European concepts in the management of Helicobacter pylori infection. The Maastricht Consensus Report. Gut. 1997;41:8-13.
48. Graham DY, Lu H, Yamaoka Y. A Report Card to Grade Helicobacter pylori Therapy. Helicobacter. 2007;12(4):275-8.
49. Malfertheiner P, Venerito M, Schulz C. Helicobacter pylori Infection: new facts in clinical management. Current treatment options in gastroenterology. 2018;16(4):605-15.
50. Malfertheiner P, Megraud F, O'Morain CA, Gisbert JP, Kuipers EJ, Axon AT, et al. Management of Helicobacter pylori infection-the Maastricht V/Florence Consensus Report. Gut. 2017;66(1):6-30.
51. Davies J, Davies D. Origins and Evolution of Antibiotic Resistance. Microbiology and Molecular Biology Reviews. 2010;74(3):417-33.
52. Frieri M, Kumar K, Boutin A. Antibiotic resistance. Journal of Infection and Public Health. 2017;10(4):369-78.
53. Organization WH. WHO publishes list of bacteria for which new antibiotics are urgently needed. 2017.
54. Smith SM. An update on the treatment of Helicobacter pylori infection. EMJ Gastroenterology. 2015;4:101-7.
55. Castro Fernandez M, Romero Garcia T, Keco Huerga A, Pabon Jaen M, Lamas Rojas E, Llorca Fernandez R, et al. Compliance, adverse effects and effectiveness of first line bismuth-containing quadruple treatment (Pylera(R)) to eradicate Helicobacter pylori infection in 200 patients. Revista espanola de enfermedades digestivas : organo oficial de la Sociedad Espanola de Patologia Digestiva. 2019;111(6):467-70.
56. Thursby E, Juge N. Introduction to the human gut microbiota. Biochemical Journal. 2017;474(11):1823-36.
57. Iebba V, Totino V, Gagliardi A, Santangelo F, Cacciotti F, Trancassini M, et al. Eubiosis and dysbiosis: the two sides of the microbiota. New Microbiol. 2016;39(1):1-12.
58. Francino MP. Antibiotics and the Human Gut Microbiome: Dysbioses and Accumulation of Resistances. Front Microbiol. 2015;6:1543.
59. Rizzatti G, Ianiro G, Gasbarrini A. Antibiotic and modulation of microbiota: a new paradigm? Journal of clinical gastroenterology. 2018;52:S74-S7.
60. Carron MA, Tran VR, Sugawa C, Coticchia JM. Identification of Helicobacter pylori biofilms in human gastric mucosa. J Gastrointest Surg. 2006;10(5):712-7.
61. Coticchia JM, Sugawa C, Tran VR, Gurrola J, Kowalski E, Carron MA. Presence and density of Helicobacter pylori biofilms in human gastric mucosa in patients with peptic ulcer disease. J Gastrointest Surg. 2006;10(6):883-9.
62. Windham IH, Servetas SL, Whitmire JM, Pletzer D, Hancock REW, Merrell DS. Helicobacter pylori Biofilm Formation Is Differentially Affected by Common Culture Conditions, and Proteins Play a Central Role in the Biofilm Matrix. Appl Environ Microbiol. 2018;84(14):e00391-18.
63. Cellini L, Grande R, Di Campli E, Traini T, Di Giulio M, Nicola Lannutti S, et al. Dynamic colonization of Helicobacter pylori in human gastric mucosa. Scandinavian Journal of Gastroenterology. 2008;43(2):178-85.
64. Vestby LK, Gronseth T, Simm R, Nesse LL. Bacterial Biofilm and its Role in the Pathogenesis of Disease. Antibiotics (Basel, Switzerland). 2020;9(2).
65. Kumar A, Alam A, Rani M, Ehtesham N, Hasnain S. Biofilms: Survival and defense strategy for pathogens. International Journal of Medical Microbiology. 2017;307.
66. Donlan RM, Costerton JW. Biofilms: survival mechanisms of clinically relevant microorganisms. Clin Microbiol Rev. 2002;15(2):167-93.
67. Costerton JW, Stewart PS, Greenberg EP. Bacterial biofilms: a common cause of persistent infections. Science. 1999;284(5418):1318-22.
68. Rodrigues C. Candida glabrata biofilms: mechanisms of antifungal resistance and matrix role 2018.
69. Yonezawa H, Osaki T, Kamiya S. Biofilm Formation by Helicobacter pylori and Its Involvement for Antibiotic Resistance. BioMed research international. 2015;2015:914791.
70. Schlafer S, Meyer RL. Confocal microscopy imaging of the biofilm matrix. Journal of microbiological methods. 2017;138:50-9.

71. Cole SP, Harwood J, Lee R, She R, Guiney DG. Characterization of monospecies biofilm formation by Helicobacter pylori. J Bacteriol. 2004;186(10):3124-32.
72. Ratthawongjirakul P, Thongkerd V, Chaicumpa W. The impacts of a fliD mutation on the biofilm formation of Helicobacter pylori. Asian Pacific Journal of Tropical Biomedicine. 2016;6(12):1008-14.
73. Branda SS, Vik Å, Friedman L, Kolter R. Biofilms: the matrix revisited. Trends in Microbiology. 2005;13(1):20-6.
74. Yonezawa H, Osaki T, Kurata S, Zaman C, Hanawa T, Kamiya S. Assessment of in vitro biofilm formation by Helicobacter pylori. Journal of Gastroenterology and Hepatology. 2010;25(s1):S90-S4.
75. Yonezawa H, Osaki T, Kurata S, Fukuda M, Kawakami H, Ochiai K, et al. Outer membrane vesicles of Helicobacter pylori TK1402 are involved in biofilm formation. BMC Microbiol. 2009;9:197.
76. Hathroubi S, Servetas SL, Windham I, Merrell DS, Ottemann KM. Helicobacter pylori Biofilm Formation and Its Potential Role in Pathogenesis. Microbiology and molecular biology reviews : MMBR. 2018;82(2).
77. Yang FL, Hassanbhai AM, Chen HY, Huang ZY, Lin TL, Wu SH, et al. Proteomannans in biofilm of Helicobacter pylori ATCC 43504. Helicobacter. 2011;16(2):89-98.
78. Stark RM, Gerwig GJ, Pitman RS, Potts LF, Williams NA, Greenman J, et al. Biofilm formation by Helicobacter pylori. Letters in Applied Microbiology. 1999;28(2):121-6.
79. Flemming HC, Wingender J. The biofilm matrix. Nat Rev Microbiol. 2010;8(9):623-33.
80. Grande R, Di Giulio M, Bessa LJ, Di Campli E, Baffoni M, Guarnieri S, et al. Extracellular DNA in Helicobacter pylori biofilm: a backstairs rumour. 2011;110(2):490-8.
81. Grande R, Di Marcantonio MC, Robuffo I, Pompilio A, Celia C, Di Marzio L, et al. Helicobacter pylori ATCC 43629/NCTC 11639 Outer Membrane Vesicles (OMVs) from Biofilm and Planktonic Phase Associated with Extracellular DNA (eDNA). Front Microbiol. 2015;6:1369.
82. Gomes B, De Martinis E. The significance of Helicobacter pylori in water, food and environmental samples. Food Control. 2004;15(5):397-403.
83. Dowsett SA, Kowolik MJ. OralHelicobacter pylori: Can We Stomach It? Critical Reviews in Oral Biology & Medicine. 2003;14(3):226-33.
84. García A, Salas-Jara MJ, Herrera C, González C. Biofilm and Helicobacter pylori: from environment to human host. World J Gastroenterol. 2014;20(19):5632-8.
85. Park SR, Mackay WG, Reid DC. Helicobacter sp. recovered from drinking water biofilm sampled from a water distribution system. Water Research. 2001;35(6):1624-6.
86. Mackay WG, Gribbon LT, Barer MR, Reid DC. Biofilms in drinking water systems: a possible reservoir for Helicobacter pylori. 1998;85(S1):52S-9S.
87. Gião MS, Azevedo NF, Wilks SA, Vieira MJ, Keevil CW. Persistence of Helicobacter pylori in heterotrophic drinking-water biofilms. Appl Environ Microbiol. 2008;74(19):5898-904.
88. Percival SL, Suleman L. Biofilms and Helicobacter pylori: Dissemination and persistence within the environment and host. World J Gastrointest Pathophysiol. 2014;5(3):122-32.
89. Moreno Y, Piqueres P, Alonso JL, Jiménez A, González A, Ferrús MA. Survival and viability of Helicobacter pylori after inoculation into chlorinated drinking water. Water research. 2007;41(15):3490-6.
90. Ng CG, Loke MF, Goh KL, Vadivelu J, Ho B. Biofilm formation enhances Helicobacter pylori survivability in vegetables. Food Microbiology. 2017;62:68-76.
91. Young KA, Akyon Y, Rampton DS, Barton S, Allaker RP, Hardie JM, et al. Quantitative culture of Helicobacter pylori from gastric juice: the potential for transmission. J Med Microbiol. 2000;49(4):343-7.
92. Young KA, Allaker RP, Hardie JM. Morphological analysis of Helicobacter pylori from gastric biopsies and dental plaque by scanning electron microscopy. Oral Microbiology and Immunology. 2001;16(3):178-81.
93. Gebara EC, Faria CM, Pannuti C, Chehter L, Mayer MP, Lima LA. Persistence of Helicobacter pylori in the oral cavity after systemic eradication therapy. J Clin Periodontol. 2006;33(5):329-33.
94. Wilson C, Lukowicz R, Merchant S, Valquier-Flynn H, Caballero J, Sandoval J, et al. Quantitative and Qualitative Assessment Methods for Biofilm Growth: A Mini-review. Res Rev J Eng Technol. 2017;6(4).
95. Ul-Hamid A. A Beginners' Guide to Scanning Electron Microscopy: Springer; 2018.
96. El Abed S, Ibnsouda SK, Latrache H, Hamadi F. Scanning electron microscopy (SEM) and environmental SEM: suitable tools for study of adhesion stage and biofilm formation. Scanning electron microscopy: Intechopen; 2012.

97. Tursunov O, Dobrowolski J, Klima K, Kordon B, Ryczkowski J, Tylko G, et al. The influence of laser biotechnology on energetic value and chemical parameters of Rose Multiflora biomass and role of catalysts for bio-energy production from biomass: Case study in Krakow-Poland. World J Environ Eng. 2015;3:58-66.
98. Lawrence JR, Neu TR. [9] Confocal laser scanning microscopy for analysis of microbial biofilms. Methods in enzymology. 310: Academic Press; 1999. p. 131-44.
99. Fellers TJ, Davidson MW. Introduction to confocal microscopy. Olympus Fluoview Resource Center. 2007.
100. Minerick AR, Thibaudeau G. Confocal Microscopy, Detection. In: Li D, editor. Encyclopedia of Microfluidics and Nanofluidics. New York, NY: Springer New York; 2015. p. 474-81.
101. Shetty A. Connecting Structure and Dynamics to Rheological Performance of Complex Fluids. 2010.
102. Nwaneshiudu A, Kuschal C, Sakamoto F, Anderson R, Schwarzenberger K, Young R. Introduction to Confocal Microscopy. The Journal of investigative dermatology. 2012;132:e3.
103. Pattiyathanee P, Vilaichone R-K, Chaichanawongsaroj N. Effect of curcumin on Helicobacter pylori biofilm formation. African Journal of Biotechnology. 2009;8:5106-15.
104. Cammarota G, Branca G, Ardito F, Sanguinetti M, Ianiro G, Cianci R, et al. Biofilm demolition and antibiotic treatment to eradicate resistant Helicobacter pylori: a clinical trial. Clin Gastroenterol Hepatol. 2010;8(9):817-20.e3.
105. Cai J, Huang H, Song W, Hu H, Chen J, Zhang L, et al. Preparation and evaluation of lipid polymer nanoparticles for eradicating H. pylori biofilm and impairing antibacterial resistance in vitro. International journal of pharmaceutics. 2015;495(2):728-37.
106. Li P, Chen X, Shen Y, Li H, Zou Y, Yuan G, et al. Mucus penetration enhanced lipid polymer nanoparticles improve the eradication rate of Helicobacter pylori biofilm. Journal of Controlled Release. 2019;300:52-63.
107. Khan I, Saeed K, Khan I. Nanoparticles: Properties, applications and toxicities. Arabian Journal of Chemistry. 2019;12(7):908-31.
108. Safarov T, Kiran B, Bagirova M, Allahverdiyev AM, Abamor ES. An overview of nanotechnology-based treatment approaches against Helicobacter Pylori. Expert Review of Anti-infective Therapy. 2019;17(10):829-40.
109. Talegaonkar S, Bhattacharyya A. Potential of Lipid Nanoparticles (SLNs and NLCs) in Enhancing Oral Bioavailability of Drugs with Poor Intestinal Permeability. AAPS PharmSciTech. 2019;20(3):121.
110. Ganesan P, Narayanasamy D. Lipid nanoparticles: Different preparation techniques, characterization, hurdles, and strategies for the production of solid lipid nanoparticles and nanostructured lipid carriers for oral drug delivery. Sustainable Chemistry and Pharmacy. 2017;6:37-56.
111. Selvamuthukumar S, Velmurugan R. Nanostructured Lipid Carriers: A potential drug carrier for cancer chemotherapy. Lipids in Health and Disease. 2012;11(1):159.
112. Üner M. Preparation, characterization and physico-chemical properties of solid lipid nanoparticles (SLN) and nanostructured lipid carriers (NLC): their benefits as colloidal drug carrier systems. Die pharmazie-an international journal of pharmaceutical sciences. 2006;61(5):375-86.
113. Naseri N, Valizadeh H, Zakeri-Milani P. Solid Lipid Nanoparticles and Nanostructured Lipid Carriers: Structure, Preparation and Application. Advanced pharmaceutical bulletin. 2015;5(3):305-13.
114. Das S, Chaudhury A. Recent Advances in Lipid Nanoparticle Formulations with Solid Matrix for Oral Drug Delivery. AAPS PharmSciTech. 2011;12(1):62-76.
115. Kim H-A, Seo J-K, Kim T, Lee B-T. Nanometrology and Its Perspectives in Environmental Research. Environmental health and toxicology. 2014;29.
116. Stetefeld J, McKenna SA, Patel TR. Dynamic light scattering: a practical guide and applications in biomedical sciences. Biophysical reviews. 2016;8(4):409-27.
117. Zhang J, Fan Y, Smith E. Experimental Design for the Optimization of Lipid Nanoparticles. Journal of Pharmaceutical Sciences. 2009;98(5):1813-9.
118. Taqvi S, Bassioni G. Understanding Wettability through Zeta Potential Measurements. Wettability and Interfacial Phenomena-Implications for Material Processing: IntechOpen; 2019.
119. Huang G, Xu B, Qiu J, Peng L, Luo K, Liu D, et al. Symmetric electrophoretic light scattering for determination of the zeta potential of colloidal systems. Colloids and Surfaces A: Physicochemical and Engineering Aspects. 2020;587:124339.

120. Kestens V, Bozatzidis V, De Temmerman P-J, Ramaye Y, Roebben G. Validation of a particle tracking analysis method for the size determination of nano-and microparticles. Journal of Nanoparticle Research. 2017;19(8):271.
121. Momen-Heravi F, Balaj L, Alian S, Tigges J, Toxavidis V, Ericsson M, et al. Alternative Methods for Characterization of Extracellular Vesicles. Frontiers in physiology. 2012;3:354.
122. Garcês A, Amaral MH, Sousa Lobo JM, Silva AC. Formulations based on solid lipid nanoparticles (SLN) and nanostructured lipid carriers (NLC) for cutaneous use: A review. European Journal of Pharmaceutical Sciences. 2018;112:159-67.
123. Battaglia L, Ugazio E. Lipid Nano- and Microparticles: An Overview of Patent-Related Research. Journal of Nanomaterials. 2019;2019:2834941.
124. Estanqueiro M, Conceição J, Amaral MH, Sousa Lobo JM. Chapter 12 - The role of liposomes and lipid nanoparticles in the skin hydration. In: Grumezescu AM, editor. Nanobiomaterials in Galenic Formulations and Cosmetics: William Andrew Publishing; 2016. p. 297-326.
125. Beloqui A, Solinís MÁ, Rodríguez-Gascón A, Almeida AJ, Préat V. Nanostructured lipid carriers: Promising drug delivery systems for future clinics. Nanomedicine: Nanotechnology, Biology and Medicine. 2016;12(1):143-61.
126. Haider M, Abdin SM, Kamal L, Orive G. Nanostructured lipid carriers for delivery of chemotherapeutics: A review. Pharmaceutics. 2020;12(3):288.
127. Wang H, Liu S, Jia L, Chu F, Zhou Y, He Z, et al. Nanostructured lipid carriers for MicroRNA delivery in tumor gene therapy. Cancer Cell International. 2018;18(1):101.
128. Zhang Q, Wu W, Zhang J, Xia X. Eradication of Helicobacter pylori: the power of nanosized formulations. Nanomedicine (Lond). 2020;15(5):527-42.
129. Correia M, Michel V, Matos AA, Carvalho P, Oliveira MJ, Ferreira RM, et al. Docosahexaenoic acid inhibits Helicobacter pylori growth in vitro and mice gastric mucosa colonization. PloS one. 2012;7(4):e35072.
130. Seabra CL, Nunes C, Gomez-Lazaro M, Correia M, Machado JC, Gonçalves IC, et al. Docosahexaenoic acid loaded lipid nanoparticles with bactericidal activity against Helicobacter pylori. International journal of pharmaceutics. 2017;519(1-2):128-37.
131. Seabra CL, Nunes C, Bras M, Gomez-Lazaro M, Reis CA, Goncalves IC, et al. Lipid nanoparticles to counteract gastric infection without affecting gut microbiota. European journal of pharmaceutics and biopharmaceutics : official journal of Arbeitsgemeinschaft fur Pharmazeutische Verfahrenstechnik eV. 2018;127:378-86.
132. Rizzato C, Torres J, Kasamatsu E, Camorlinga-Ponce M, Bravo MM, Canzian F, et al. Potential Role of Biofilm Formation in the Development of Digestive Tract Cancer With Special Reference to Helicobacter pylori Infection. Frontiers in Microbiology. 2019;10(846).
133. Wong EHJ, Ng CG, Goh KL, Vadivelu J, Ho B, Loke MF. Metabolomic analysis of low and high biofilm-forming Helicobacter pylori strains. Scientific Reports. 2018;8(1):1409.
134. Loh JT, Torres VJ, Scott Algood HM, McClain MS, Cover TL. Helicobacter pylori HopQ outer membrane protein attenuates bacterial adherence to gastric epithelial cells. FEMS microbiology letters. 2008;289(1):53-8.
135. Shao C, Sun Y, Wang N, Yu H, Zhou Y, Chen C, et al. Changes of proteome components of Helicobacter pylori biofilms induced by serum starvation. Molecular Medicine Reports. 2013;8(6):1761-6.
136. CLSI. Methods for Determining Bactericidal Activity of Antimicrobial Agents; Approved Guideline. M26-A. Clin Lab Stand Inst. 1999;19:7.
137. Seabra CL, Nunes C, Gomez-Lazaro M, Correia M, Machado JC, Goncalves IC, et al. Docosahexaenoic acid loaded lipid nanoparticles with bactericidal activity against Helicobacter pylori. International journal of pharmaceutics. 2017;519(1-2):128-37.
138. Macia MD, Rojo-Molinero E, Oliver A. Antimicrobial susceptibility testing in biofilm-growing bacteria. Clinical Microbiology and Infection. 2014;20(10):981-90.
139. Lee Y-C, Chiang T-H, Chou C-K, Tu Y-K, Liao W-C, Wu M-S, et al. Association Between Helicobacter pylori Eradication and Gastric Cancer Incidence: A Systematic Review and Meta-analysis. Gastroenterology. 2016;150(5):1113-24.e5.
140. Rawla P, Barsouk A. Epidemiology of gastric cancer: global trends, risk factors and prevention. Prz Gastroenterol. 2019;14(1):26-38.
141. Thung I, Aramin H, Vavinskaya V, Gupta S, Park JY, Crowe SE, et al. Review article: the global emergence of Helicobacter pylori antibiotic resistance. Alimentary Pharmacology & Therapeutics. 2016;43(4):514-33.

142. Yonezawa H, Osaki T, Hojo F, Kamiya S. Effect of Helicobacter pylori biofilm formation on susceptibility to amoxicillin, metronidazole and clarithromycin. Microbial pathogenesis. 2019;132:100-8.
143. Desbois AP, Smith VJ. Antibacterial free fatty acids: activities, mechanisms of action and biotechnological potential. Applied microbiology and biotechnology. 2010;85(6):1629-42.
144. Taneja A, Singh H. Challenges for the Delivery of Long-Chain n-3 Fatty Acids in Functional Foods. Annual Review of Food Science and Technology. 2012;3(1):105-23.
145. Date AA, Hanes J, Ensign LM. Nanoparticles for oral delivery: Design, evaluation and state-of-the-art. Journal of Controlled Release. 2016;240:504-26.
146. Fulaz S, Vitale S, Quinn L, Casey E. Nanoparticle–Biofilm Interactions: The Role of the EPS Matrix. Trends in Microbiology. 2019;27(11):915-26.
147. Liu Y, Shi L, Su L, van der Mei HC, Jutte PC, Ren Y, et al. Nanotechnology-based antimicrobials and delivery systems for biofilm-infection control. Chemical Society Reviews. 2019;48(2):428-46.
148. Samimi S, Maghsoudnia N, Eftekhari RB, Dorkoosh F. Chapter 3 - Lipid-Based Nanoparticles for Drug Delivery Systems. In: Mohapatra SS, Ranjan S, Dasgupta N, Mishra RK, Thomas S, editors. Characterization and Biology of Nanomaterials for Drug Delivery: Elsevier; 2019. p. 47-76.
149. Benoit DSW, Sims KR, Jr., Fraser D. Nanoparticles for Oral Biofilm Treatments. ACS Nano. 2019;13(5):4869-75.
150. Rabin N, Zheng Y, Opoku-Temeng C, Du Y, Bonsu E, Sintim HO. Biofilm formation mechanisms and targets for developing antibiofilm agents. Future Medicinal Chemistry. 2015;7(4):493-512.
151. McBain AJ. Chapter 4 In Vitro Biofilm Models: An Overview. Advances in Applied Microbiology. 69: Academic Press; 2009. p. 99-132.
152. Hortelano I, Moreno Y, Vesga FJ, Ferrús MA. Evaluation of different culture media for detection and quantification of H. pylori in environmental and clinical samples. International Microbiology. 2020;23(4):481-7.
153. Jiménez-Soto LF, Rohrer S, Jain U, Ertl C, Sewald X, Haas R. Effects of Cholesterol on Helicobacter pylori Growth and Virulence Properties In Vitro. Helicobacter. 2012;17(2):133-9.
154. Taraszkiewicz A, Fila G, Grinholc M, Nakonieczna J. Innovative Strategies to Overcome Biofilm Resistance. BioMed research international. 2013;2013:150653.
155. Kumar P, Lee J-H, Beyenal H, Lee J. Fatty Acids as Antibiofilm and Antivirulence Agents. Trends in Microbiology. 2020;28(9):753-68.
156. Dinicola S, De Grazia S, Carlomagno G, Pintucci J. N-acetylcysteine as powerful molecule to destroy bacterial biofilms. A systematic review. Eur Rev Med Pharmacol Sci. 2014;18(19):2942-8.
157. ThermoScientific™. FilmTracer™ LIVE/DEAD® Biofilm Viability Kit. In: Invitrogen, editor. 2009.
158. Rosenberg M, Azevedo NF, Ivask A. Propidium iodide staining underestimates viability of adherent bacterial cells. Sci Rep. 2019;9(1):6483.
159. Logan RP, Walker MM. ABC of the upper gastrointestinal tract: Epidemiology and diagnosis of Helicobacter pylori infection. BMJ: British Medical Journal. 2001;323(7318):920.
160. Patra R, Chattopadhyay S, De R, Ghosh P, Ganguly M, Chowdhury A, et al. Multiple infection and microdiversity among Helicobacter pylori isolates in a single host in India. PloS one. 2012;7(8):e43370.

Appendix I - Poster communication at i3S annual meeting 2019

P164

POSTER COMMUNICATION

Specificity of lipid nanoparticles against *Helicobacter pylori*

A. S. Pinho[1,2,3,4], C. Nunes[5], S. Reis[5], M. C. Martins[1,2], C. L. Seabra[6], P. Parreira[1,2]

[1]i3S - Instituto de Investigação e Inovação em Saúde, Universidade do Porto, Portugal; [2]BioEngineered Surfaces, INEB – Instituto de Engenharia Biomédica, Portugal; [3]FEUP – Faculdade de Engenharia da Universidade do Porto, Portugal; [4]ICBAS – Instituto de Ciência Biomédicas Abel Salazar, Portugal; [5]LAQV, REQUIMTE, Laboratório de Química Aplicada, Faculdade de Farmácia da Universidade do Porto, Portugal; [6]CBQF - Centre for Biotechnology and Fine Chemistry, Universidade Católica Portuguesa, Porto, Portugal.

Helicobacter pylori (*Hp*) is a bacterium found in the stomach of half of the world's population (≈4 billion people) [1]. *Hp* infection is the primary known cause for the development of gastric disorders, such as gastritis, gastroduodenal ulcers and gastric cancer [2]. The available therapeutic regimen based on antibiotics fails in ~40% of cases, mainly due to high antibiotic resistance rates [3]. Moreover, antibiotics are not selective, promoting dysbiosis, an unbalance and change of gut microbiota, influencing the human body physiologic processes [4]. Therefore, it is important to develop a nanodelivery system able to inhibit and kill *Hp*, but also, "friendly" to gut microbiota.

Previously, lipid nanoparticles (unloaded and docosahexaenoic acid loaded nanostructured lipid carriers, NLC and DHA-NLC) were described as effective against a human *Hp* strain (J99), killing *Hp* in a concentration and time dependent way [5, 6]. Since gastric infection is characteristically multi-strain, the aim of this work was to establish their effectiveness against other human Hp strains (*Hp* ATCC® 26695 and *Hp* NCTC 11637). Also, their effect upon gut microbiota was accessed using representative bacteria strains of normal (*Bifidobacterium longum* CIP 64.62, *B. breve* NCIMB® 702258, *B. animalis* subsp. *lactis* BB-12®, *B. adolescentis* DSMZ® 20083 and *Lactobacillus acidophilus* LA-5®) and dysbiotic microbiota (*Pseudomonas aeruginosa* ATCC® 27853ô, *Staphylococcus aureus* ATCC® 33591ô, *Escherichia coli* ATCC® 25922ô, clinical isolates of *Enterococcus faecalis* and *Salmonella sp* (*enteric*)).

The lipid nanoparticles were produced by hot homogenization and ultrasonication using a blend of lipids (Miglyol®812 and Precirol® ATO5) and a surfactant (Tween® 60). They were characterized in terms of size, showing an average of 221±2.7 and 255±1.0 nm, and surface charge, with an average of -31±0.8 mV and -27±0.6 mV, for NLC and DHA-NLC, respectively. *In vitro* activity of the lipid nanoparticles towards different *Hp* strains and bacteria from gut microbiota (normal and dysbiotic) was assessed by determination of minimal inhibitory concentration (MIC) and minimal bactericidal concentration (MBC) using the microbroth dilution method [7]. Our findings showed that the lipid nanoparticles were able to inhibit *Hp* growth at 0.31% v/v and have a bactericidal effect in the 0.31-1.25% v/v range. Moreover,

the tested lipid nanoparticles did not harm bacteria from the healthy gut microbiota, showing specificity towards the gastric pathogen.

In conclusion, lipid nanoparticles should be considered as an antibiotic-free, microbiota friendly alternative treatment for *H. pylori* infection.

References
[1] Eslami M., *et al.*, J. Cell Physiol., 2019.
[2] Molnar B., *et al.*, Dig. Dis., 2010.
[3] Malfertheiner P., *et al.*, Gut, 2017.
[4] Rizzatti G., *et al.*, J. Clin. Gastroenterol., 2018.
[5] Seabra C.L., *et al.*, Int. J. Pharm., 2017.
[6] Seabra C.L., *et al.*, Eur. J. Pharm. Biopharm., 2018.
[7] Wiegand I., *et al.*, Nat. Protoc., 2008.

Specificity of lipid nanoparticles against *Helicobacter pylori*

A. S. Pinho [1,2,3,4], C. Nunes [5], S. Reis [5], M. C. L. Martins [1,2], C. L. Seabra [6], P. Parreira [1,2]

[1]i3S - Instituto de Investigação e Inovação em Saúde, Universidade do Porto, Portugal; [2]BioEngineered Surfaces, INEB - Instituto de Engenharia Biomédica, Portugal; [3]FEUP - Faculdade de Engenharia da Universidade do Porto, Portugal; [4]ICBAS - Instituto de Ciência Biomédicas Abel Salazar, Portugal; [5]LAQV, REQUIMTE, Laboratório de Química Aplicada, Faculdade de Farmácia da Universidade do Porto, Portugal; [6] Universidade Católica Portuguesa, CBQF - Centro de Biotecnologia e Química Fina - Laboratório Associado, Escola Superior de Biotecnologia, Porto, Portugal.

Helicobacter pylori colonizes the stomach of half of the world's population (≈4 billion people) [1]. *H. pylori* infection is linked with development of gastric disorders, such as gastritis, gastroduodenal ulcers and gastric cancer [2]. The available therapeutic regimen based on antibiotics fails in ≈40% of cases, mainly due to high antibiotic resistance rates [3]. Moreover, antibiotics are not selective, promoting dysbiosis, an unbalance and change of gut microbiota, influencing the human body physiologic processes [4].It is important to develop a strategy able to eradicate *H. pylori* that is also "friendly" to gut microbiota. Previously, lipid nanoparticles (unloaded and docosahexaenoic acid loaded nanostructured lipid carriers, NLC and DHA-NLC, respectively) were described as effective against a human *H. pylori* strain (J99) [5, 6].

AIMS: (i) to establish NLC and DHA-NLC effectiveness against other human *H. pylori* strains, since infection is characteristically multi-strain; (ii) evaluate NLC and DHA-NLC effect upon gut microbiota (normal and dysbiotic).

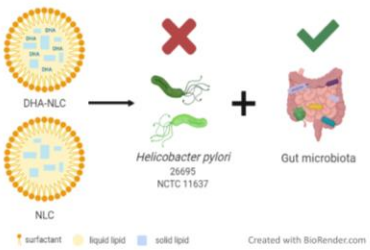

Preparation and characterization of NLC and DHA-NLC

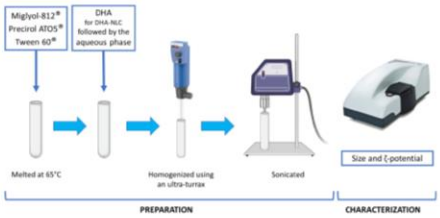

Figure 1. Schematic representation of NLC and DHA-NLC production.

Table 1. Nanoparticle characterization.

	Size (nm)	ζ-potential (mV)	Polydispersity index
NLC	221±2.7	-31±0.8	0.19
DHA-NLC	255±1.0	-27±0.6	0.16

- These results are in agreement with previous experiments [5].
- The low polydispersity index indicates homogeneous size distribution.

In vitro testing (MIC and MBC determination)

H. pylori and microbiota strains were cultured as described [5,7].

Minimal Inhibitory Concentration (MIC) and the Minimal Bactericidal Concentration (MBC) assays adapted from Clinical and Laboratory Standards Institute (CLSI) guidelines and using the microbroth dilution method [8,9].

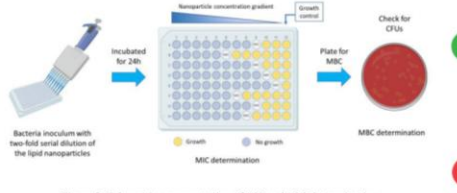

Figure 2. Schematic representation of MIC and MBC determination.

Table 2. MIC and MBC assay results.

		MIC (%v/v)	MBC (%v/v)
Helicobacter pylori 26695	NLC	0.3125	0.3125 – 0.6
	DHA-NLC	0.3125 (6.25μM)	0.3125 (6.25μM)
Helicobacter pylori NCTC 11637	NLC	0.3125	0.3125 – 1.25
	DHA-NLC	0.3125 (6.25μM)	0.3125 (6.25μM)
Bifidobacterium longum CIP 64.62	NLC	> 40 (800 μM)	-
	DHA-NLC	> 40 (800 μM)	-
Bifidobacterium breve NCIMB® 702258	NLC	> 40 (800 μM)	-
	DHA-NLC	> 40 (800 μM)	-
Bifidobacterium animalis subsp. *lactis* BB-12®	NLC	> 40 (800 μM)	-
	DHA-NLC	> 40 (800 μM)	-
Bifidobacterium adolescentis DSM2® 20083	NLC	> 40 (800 μM)	-
	DHA-NLC	> 40 (800 μM)	-
Lactobacillus acidophilus LA-5®	NLC	> 40 (800 μM)	-
	DHA-NLC	> 40 (800 μM)	-
Pseudomonas aeruginosa ATCC® 27853™	NLC	> 40 (800 μM)	-
Staphylococcus aureus ATCC® 33591™	NLC	5 (100 μM)	10 (200 μM)
Escherichia coli ATCC® 25922™	NLC	> 40 (800 μM)	-
clinical isolates of *Enterococcus faecalis*	NLC	> 40 (800 μM)	-
clinical isolates of *Salmonella sp (enteric)*	NLC	> 40 (800 μM)	-

- NLC and DHA-NLC showed inhibitory and bactericidal effect against *H. pylori*.
- NLC and DHA-NLC had no bactericidal effect in most of the tested bacteria at the highest concentration tested - 40% v/v (800 μM of DHA).

Normal microbiota

Dysbiotic microbiota

Conclusions

- NLC and DHA-NLC were bactericidal against a panel of human *H. pylori* strains, increasing its potential for the treatment of multi strain gastric infection.
- The specificity of these nanoparticles for *H. pylori* is a huge advantage, since unlike antibiotic therapy, it will allow the preservation of the gut microbiota.

NLCs and DHA-NLCs have high therapeutic potential and should be pursued as a treatment for *H. pylori* infection.

References

1. Eslami, M., *et al.* J Cell Physiol, 2019.
2. Molnar, B., *et al.*, Dig Dis, 2010.
3. Malfertheiner, P., *et al.*, Gut, 2017.
4. Rizzatti, G., *et al.* J Clin Gastroenterol, 2018.
5. Seabra, C.L., *et al.*. Int J Pharm, 2017.
6. Seabra, C.L., *et al.* Eur J Pharm Biopharm, 2018.
7. Sousa S. *et al.* Eng. Life Sci. 2012, 12, No. 4, 457-465
8. Patel, J., *et al.*,*CLSI M100-S25*. 2015.
9. Wiegand, I., *et al.*. Nat Protoc, 2008.

Acknowledgments

This work was supported by FEDER - Fundo Europeu de Desenvolvimento Regional funds through the COMPETE 2020 - Operational Program for Competitiveness and Internationalization (POCI), Portugal 2020 and NORTE-01-0145-FEDER-000012 and by FCT - Fundação para a Ciência e a Tecnologia/Ministério da Ciência, Tecnologia e Inovação through the POCI-01-0145-FEDER-007274, PyloriBinders - Helicobacter pylori specific biomaterials for antibiotic-free treatment/diagnostic of gastric infection (PTDC/CTM-BIO/4043/2014) UID/QUI/50006/2013 (LAQV-REQUIMTE) projects.

The authors acknowledge the former and present members of the BioEngineered Surfaces group at i3s and the Molecular Biophysics and Biotechnology group at FFUP that contributed to this work, as well as the Universidade Católica Portuguesa, CBQF- Centro de Biotecnologia e Química Fina for supplying the *Bifidobacterium* spp. and *L. acidophilus* strains and its facilities for performing assays in anaerobic conditions.

INSTITUTO
DE INVESTIGAÇÃO
E INOVAÇÃO
EM SAÚDE
UNIVERSIDADE
DO PORTO

Rua Alfredo Allen, 208
4200-135 Porto
Portugal
+351 220 408 800

www.i3s.up.pt

Appendix II - Oral communication at Encontro de Investigação Jovem da Universidade do Porto (IJUP) 2020

- 16945 | Fighting Helicobacter pylori: a specific antibiotic-free strategy

Pinho, A. S., Faculdade de Engenharia da Universidade do Porto, Portugal
Nunes, C., LAQV, Portugal
Reis, S., LAQV, Portugal
Martins, M. C. L., I3S, Portugal
Seabra, C. L., CBQF - UCP, Portugal
Parreira, P., I3S, Portugal

Helicobacter pylori (Hp) infection is associated with development of gastric disorders, namely gastric cancer [1]. The available antibiotic therapy fails in ~40% of cases and is not selective, promoting dysbiosis [2,3]. So, a strategy able to kill *Hp* while being "friendly" to gut microbiota, is crucial.
Lipid nanoparticles, namely nanostructured lipid carriers (NLC) and docosahexaenoic acid loaded NLC (DHA-NLC), were effective against a human *Hp* strain (J99) [4,5]. Since gastric infection is characteristically multi-strain, we aimed to establish the nanoparticles effectiveness against other human *Hp* strains (*Hp* ATCC® 26695; *Hp* NCTC 11637). Effect upon normal and dysbiotic gut microbiota, was also evaluated.
They were produced and characterized as previously described by us [4]. *In vitro* activity of nanoparticles was assessed by determination of minimal inhibitory concentration and minimal bactericidal concentration using the microbroth dilution method [6]. Our findings showed that NLC inhibited both *Hp* strains growth at 0.31% v/v and were bactericidal in the 0.31-1.25% v/v range, while DHA-NLC inhibited and killed both strains at 0.31% v/v. These nanoparticles did not harm bacteria from the normal or dysbiotic gut microbiota.
The developed nanoparticles are bactericidal against *Hp* in a specific way since they do not affect other bacteria from gut microbiota. Altogether, this microbiota "friendly" strategy should be considered as an antibiotic-free alternative for gastric infection treatment.

Acknowledgements: UID/BIM/04293/2019/, PTDC/CTM-BIO/4043/2014, UID/QUI/50006/2013 (LAQV-REQUIMTE), PTDC/BAA-AGR/31400/2017 and UID/Multi/50016/2019 projects.
References: 1. Molnar B., et al., 2010; 2. Malfertheiner P., et al., 2017; 3. Rizzatti G., et al., 2018; 4. Seabra C.L., et al., 2017; 5. Seabra C.L., et al., 2018; 6. Wiegand I., et al., 2008.

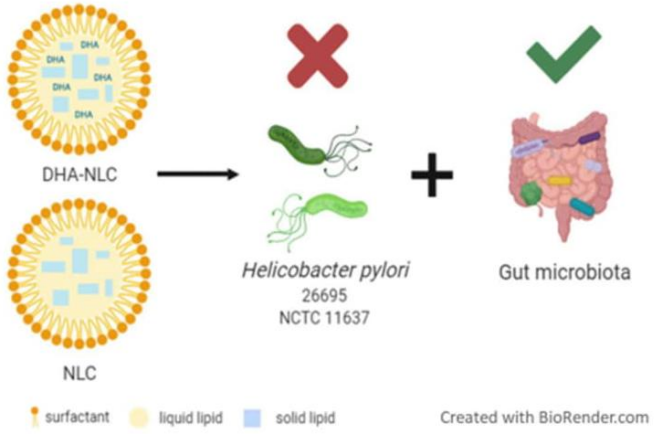

Graphical abstract